QED calculation of the $n=1$ and $n=2$ energy levels in He-like ions

A. N. Artemyev,[1,2] V. M. Shabaev,[1,2] V. A. Yerokhin,[1,2,3] G. Plunien,[2] and G. Soff[2]
[1]*Department of Physics, St. Petersburg State University, Oulianovskaya 1, Petrodvorets, St. Petersburg 198504, Russia*
[2]*Institut für Theoretische Physik, TU Dresden, Mommsenstraße 13, D-01062 Dresden, Germany*
[3]*Center for Advanced Studies, St. Petersburg State Polytechnical University, Polytekhnicheskaya 29, St. Petersburg 195251, Russia*
(Received 14 January 2005; published 21 June 2005)

We perform *ab initio* QED calculations of energy levels for the $n=1$ and $n=2$ states of He-like ions with the nuclear charge in the range $Z=12$–100. The complete set of two-electron QED corrections is evaluated to all orders in the parameter αZ. Uncalculated contributions to energy levels come through orders $\alpha^3(\alpha Z)^2$, $\alpha^2(\alpha Z)^7$, and higher. A significant improvement in accuracy of theoretical predictions is achieved, especially in the high-Z region.

DOI: 10.1103/PhysRevA.71.062104 PACS number(s): 12.20.Ds, 31.30.Jv, 31.10.+z

Introduction

Helium and heliumlike ions, being the simplest many-electron systems, traditionally serve as an important testing ground for investigations of many-body relativistic and QED effects. Calculations of QED effects in He-like ions have a long history. The expression for the Lamb shift complete through orders $\alpha(\alpha Z)^4$ and $\alpha^2(\alpha Z)^3$ was derived in pioneering studies by Araki [1] and Sucher [2]. Numerous subsequent investigations of higher-order QED corrections in two-electron systems (see, e.g., the review [3] and recent original studies [4–6]) were primarily aimed at helium, in which the experimental accuracy is by far better than in other two-electron systems. Recent progress in experimental spectroscopy of highly charged ions [7–9] opened perspectives for probing higher-order QED effects in ions along the helium isoelectronic sequence up to He-like uranium. Investigations of QED effects in high-Z ions are of particular importance since they can provide tests of quantum electrodynamics in the region of a very strong Coulomb field of the nucleus. Another factor that stimulates these investigations is the possibility to test the standard model by studying the effects of parity nonconservation (PNC) [10–13]. Experimental identification of the PNC effects will require precise knowledge of the $2\,{}^1S_0$–$2\,{}^3P_0$ interval in He-like ions with nuclear charge numbers near $Z=64$ (gadolinium) and 90 (thorium), which happens to be very small for these values of Z, thus enhancing the PNC effects significantly.

Investigations of QED effects in heavy He-like ions differ significantly from those for the helium atom. First of all, the nuclear coupling parameter αZ approaches unity and cannot be regarded as a good expansion parameter as in the case of helium. But on the other side, the electron-electron interaction in these systems is suppressed by a factor of $1/Z$ with respect to the electron-nucleus interaction and, therefore, can be accounted for by a perturbation expansion in the parameter $1/Z$.

Until recently, the only QED effects calculated to all orders in αZ were the one-electron self-energy and vacuum-polarization corrections [14,15]. So theoretical investigations of energy levels in heavy He-like ions mostly relied on these one-electron values [16]. For medium-Z ions, hydrogenic QED effects were corrected for the "screening" by various semiempirical rules, notably, within Welton's approximation, as in Ref. [17]. A more elaborate treatment of QED effects in He-like ions was presented by Drake [18]. His values for the QED correction included the complete contribution to order $\alpha^2(\alpha Z)^3$ derived in Refs. [1,2] and parts of higher-order contributions obtained by employing the all-order results available for the one-electron QED corrections. The total energy values of Ref. [18] are complete through order $\alpha^2(\alpha Z)^3$ and uncalculated terms start at orders $\alpha^2(\alpha Z)^4$ and $\alpha^3(\alpha Z)^2$.

Later, Johnson and Sapirstein [19] applied relativistic many-body perturbation theory (MBPT) to the treatment of the electron correlation for $n=2$ triplet states of He-like ions. Combined with Drake's values for the QED and recoil corrections, their results yielded a better agreement with the experimental data than those of Ref. [18]. While the approach of Ref. [19] is still incomplete to order $\alpha^2(\alpha Z)^4$, it includes terms that were not accounted for in Ref. [18], namely, the Breit-Breit interaction and some relativistic corrections to the second-order energy. Later, other evaluations of the electron-correlation part of the energies of He-like ions were performed by the relativistic configuration-interaction (CI) method [20], by the relativistic all-order MBPT approach [21], and by the multiconfigurational Dirac-Fock method [22]. The studies [19–21] share the same main features: their treatment is based on the no-pair Hamiltonian and the electron correlation is taken into account within the Breit approximation. The results of these evaluations are in a very good agreement with each other.

A somewhat different approach was employed in Refs. [23,24]. While the electron-correlation part was evaluated (as in the previous work by the same group [20]) by the CI method, the QED part was not taken from Ref. [18] but evaluated independently, by considering the one-loop QED corrections in a local screening potential. Due to different treatments of QED effects, there are certain deviations between the results of Refs. [23,24] and those of Refs. [19–21].

In order to obtain reliable predictions for energy levels of high-Z ions and to improve the theoretical accuracy in the low- and middle-Z region, it is necessary to take into account two-electron QED effects without an expansion in αZ. Such a project has been recently accomplished (up to order α^2) for

the two-electron part of the ground-state energy of He-like ions [25–29] and for the lowest-lying states of Li-like ions [30–33]. To perform similar QED calculations for excited states of He-like ions is more difficult. One of the reasons is that we encounter levels that are quasidegenerate, namely, $2\,^3P_1$ and $2\,^1P_1$. To derive formal expressions for QED corrections in case of quasidegenerate states is a serious problem that was solved first within the two-time Green's function (TTGF) method [34–36]. Different approaches to this problem have recently been addressed by other authors [37,38].

Several QED corrections have been calculated to all orders in αZ for excited states of He-like ions up to now. In our previous investigation [39], we evaluated the vacuum-polarization screening correction for all $n=2$ states of He-like ions. The two-photon exchange correction was calculated for excited states of He-like ions by Mohr and Sapirstein [40] ($2\,^3S_1$ and $2\,^3P_{0,2}$ states), by Andreev *et al.* [41,42] ($2\,^1S_{0,1}, 2\,^3P_0$) and [38] ($2\,^{1,3}P_1$), and by Åsen *et al.* [43] ($2\,^1S_{0,1}$). The self-energy screened by a spherically symmetric part of the electron-electron interaction was calculated by Indelicato and Mohr [44]. In this paper we present a rigorous evaluation of the self-energy screening correction and an independent calculation of the two-photon exchange correction for all $n=2$ states of He-like ions. This completes the *ab initio* treatment of all *two-electron* QED corrections of order α^2 to all orders in αZ and significantly improves the theoretical accuracy for the energy values, especially in the high-Z region. Unlike previous calculations, the results obtained are complete through order $\alpha^2(\alpha Z)^4$; uncalculated terms enter through three-photon QED effects [to order $\alpha^3(\alpha Z)^2$ and higher] and through two-loop one-electron QED corrections [$\alpha^2(\alpha Z)^7$ and higher].

The paper is organized as follows. In the next section we describe the basic formalism and present general formulas for the two-electron QED corrections for the case of quasidegenerate levels. In Sec. II, the numerical procedure is briefly discussed and numerical results are presented for the two-photon exchange correction and the screened self-energy correction. The total two-electron QED correction is then compiled, analyzed, and compared with the known terms of the αZ expansion. In the last section, we present a compilation of all contributions available to the energy levels and compare results of different theoretical evaluations with existing experimental data. Relativistic units ($\hbar=c=m=1$) are used throughout the paper.

I. FORMAL EXPRESSIONS

A. Basic formalism

In this section we briefly formulate the basic equations of the TTGF method for quasidegenerate states of a He-like ion. A detailed description of the method and, particularly, its implementation for the case of quasidegenerate states can be found in Refs. [35,36,45]. The derivation will be given for two particular quasidegenerate states $(1s2p_{1/2})_1$ and $(1s2p_{3/2})_1$ and can immediately be extended to a more general case. The unperturbed two-electron wave functions in the jj coupling are given by

$$u_1 = \sum_{m_a m_v} \langle j_a m_a j_v m_v | JM \rangle \frac{1}{\sqrt{2}} \sum_P (-1)^P |PaPv\rangle, \qquad (1)$$

$$u_2 = \sum_{m_a m_w} \langle j_a m_a j_w m_w | JM \rangle \frac{1}{\sqrt{2}} \sum_P (-1)^P |PaPw\rangle, \qquad (2)$$

where a, v, and w are taken to represent $1s, 2p_{1/2}$, and $2p_{3/2}$ orbitals, respectively; P is the permutation operator

$$\sum_P (-1)^P |P_a P_v\rangle = |av\rangle - |va\rangle,$$

and $|av\rangle \equiv |a\rangle|v\rangle$ is the product of the one-electron Dirac wave functions. The transition to the wave functions corresponding to the LS-coupling scheme within the nonrelativistic approximation can be performed by

$$\begin{pmatrix} |2\,^3P_1\rangle \\ |2\,^1P_1\rangle \end{pmatrix} = R \begin{pmatrix} |(1s2p_{1/2})_1\rangle \\ |(1s2p_{3/2})_1\rangle \end{pmatrix}, \qquad (3)$$

with

$$R = \frac{1}{\sqrt{3}} \begin{pmatrix} \sqrt{2} & -1 \\ 1 & \sqrt{2} \end{pmatrix}. \qquad (4)$$

We mention that this choice of the matrix R implies that the one-electron $2p_{1/2}$ and $2p_{3/2}$ wave functions have the same sign in the nonrelativistic limit.

In order to introduce the two-time Green's function which is needed to formulate the method, it is convenient to start with the standard definition of the four-time two-electron Green's function in the external field of the nucleus

$$G(x_1', x_2'; x_1, x_2) = \langle 0 | T \psi(x_1') \psi(x_2') \bar{\psi}(x_1) \bar{\psi}(x_2) | 0 \rangle, \qquad (5)$$

where $\psi(x)$ is the electron-positron field operator in the Heisenberg representation, $\bar{\psi} = \psi^\dagger \gamma^0$, and T denotes the time-ordered product operator. This Green's function is constructed by perturbation theory after the transition to the interaction representation where it is given by (see, e.g., [46])

$$G(x_1', x_2'; x_1, x_2) = \frac{\langle 0 | T \psi_{\rm in}(x_1') \psi_{\rm in}(x_2') \bar{\psi}_{\rm in}(x_2) \bar{\psi}_{\rm in}(x_1) \exp[-i \int d^4z\, \mathcal{H}_{\rm int}(z)] | 0 \rangle}{\langle 0 | T \exp[-i \int d^4z\, \mathcal{H}_{\rm int}(z)] | 0 \rangle}. \qquad (6)$$

Here $\psi_{\rm in}(x)$ is the electron-positron field operator in the interaction representation and $\mathcal{H}_{\rm int}$ is the interaction Hamiltonian. Expression (6) allows one to construct G by using Wick's theorem.

The corresponding Green's function in the mixed energy-coordinate representation is defined by

$$G(p'^0_1,\mathbf{x}'_1,p'^0_2,\mathbf{x}'_2;p^0_1,\mathbf{x}_1,p^0_2,\mathbf{x}_2) = \frac{1}{(2\pi)^4}\int_{-\infty}^{\infty} dx^0_1 dx^0_2 dx'^0_1 dx'^0_2 \times \exp(ip'^0_1 x'^0_1 + ip'^0_2 x'^0_2 - ip^0_1 x^0_1 - ip^0_2 x^0_2) G(x'_1,x'_2;x_1,x_2). \tag{7}$$

The Feynman rules for $G(p'^0_1,\mathbf{x}'_1,p'^0_2,\mathbf{x}'_2;p^0_1,\mathbf{x}_1,p^0_2,\mathbf{x}_2)$ can be found in [36,45]. We now introduce the Green's function $g(E)$ as

$$g(E)\delta(E-E') = \frac{\pi}{i}\int_{-\infty}^{\infty} dp^0_1 dp^0_2 dp'^0_1 dp'^0_2 \delta(E-p^0_1-p^0_2) \times \delta(E'-p'^0_1-p'^0_2) P_0 G(p'^0_1,p'^0_2;p^0_1,p^0_2)\gamma^0_1\gamma^0_2 P_0, \tag{8}$$

where $P_0=\Sigma_k u_k u_k^\dagger$ is the projector on the subspace of the unperturbed quasidegenerate states under consideration [see Eqs. (1) and (2)]. It can easily be shown (see, e.g., Refs. [36,45]) that the Green's function g is the Fourier transform of the two-time Green's function projected on the subspace of the unperturbed quasidegenerate states.

It can be derived (see Ref. [36] for details) that the system under consideration can be described by a two-dimensional Schrödinger-like equation ($k=1,2$),

$$H\psi_k = E_k\psi_k, \quad \psi_k^\dagger\psi_{k'} = \delta_{kk'}, \tag{9}$$

where

$$H = P^{-1/2}KP^{-1/2}, \tag{10}$$

$$K = \frac{1}{2\pi i}\oint_\Gamma dE\, E\, g(E), \tag{11}$$

$$P = \frac{1}{2\pi i}\oint_\Gamma dE\, g(E). \tag{12}$$

Γ is a contour in the complex E plane that surrounds the levels under consideration but does not encircle other levels, and E_k are the exact energies of the states under consideration. It is assumed that the contour Γ is oriented counterclockwise. The operator H, which is a 2×2 matrix, is constructed by perturbation theory in α. Substituting

$$g(E) = g^{(0)}(E) + g^{(1)}(E) + g^{(2)}(E) + \cdots, \tag{13}$$

$$P = P^{(0)} + P^{(1)} + P^{(2)} + \cdots, \tag{14}$$

$$K = K^{(0)} + K^{(1)} + K^{(2)} + \cdots, \tag{15}$$

where the superscript indicates the order in α, we obtain [35]

$$H^{(0)} = K^{(0)}, \tag{16}$$

$$H^{(1)} = K^{(1)} - \frac{1}{2}P^{(1)}K^{(0)} - \frac{1}{2}K^{(0)}P^{(1)}, \tag{17}$$

$$H^{(2)} = K^{(2)} - \frac{1}{2}P^{(2)}K^{(0)} - \frac{1}{2}K^{(0)}P^{(2)} - \frac{1}{2}P^{(1)}K^{(1)} - \frac{1}{2}K^{(1)}P^{(1)} + \frac{3}{8}P^{(1)}P^{(1)}K^{(0)} + \frac{3}{8}K^{(0)}P^{(1)}P^{(1)} + \frac{1}{4}P^{(1)}K^{(0)}P^{(1)}. \tag{18}$$

The solvability of Eq. (9) yields the basic equation for the calculation of the energy levels

$$\det(E-H) = 0. \tag{19}$$

As was noticed in Ref. [35], due to nonzero decay rates of excited states, the self-adjoint part of H should be understood in Eqs. (9) and (19),

$$H \equiv (1/2)(H+H^\dagger). \tag{20}$$

To zeroth order in α, the Green's function $g(E)$ is

$$g^{(0)}(E) = \sum_{s=1}^{2}\frac{|u_s\rangle\langle u_s|}{E-E_s^{(0)}}, \tag{21}$$

where $E_1^{(0)}$ and $E_2^{(0)}$ are the unperturbed energies of the $(1s2p_{1/2})_1$ and $(1s2p_{3/2})_1$ states, respectively, given by the sum of the one-electron Dirac-Coulomb energies:

$$E_1^{(0)} = \varepsilon_{1s} + \varepsilon_{2p_{1/2}}, \quad E_2^{(0)} = \varepsilon_{1s} + \varepsilon_{2p_{3/2}}.$$

Substituting Eq. (21) into the definitions of K,P, and H, one gets

$$K^{(0)}_{ik} = E^{(0)}_i\delta_{ik}, \tag{22}$$

$$P^{(0)}_{ik} = \delta_{ik}, \tag{23}$$

$$H^{(0)}_{ik} = E^{(0)}_i\delta_{ik}. \tag{24}$$

Now we introduce a set of notations that will shorten the following expressions. The shorthand notation will be used for the summation over the Clebsch-Gordan coefficients in Eqs. (1) and (2):

$$F_i|i_1i_2\rangle \equiv \sum_{m_{i_1}m_{i_2}}\langle j_{i_1}m_{i_1}j_{i_2}m_{i_2}|JM\rangle|i_1i_2\rangle, \tag{25}$$

where $|i_1i_2\rangle$ is either $|av\rangle$ or $|aw\rangle$. It is convenient also to use the notation for the operator of the electron-electron interaction:

$$I(\omega) = e^2\alpha_1^\mu\alpha_2^\nu D_{\mu\nu}(\omega), \tag{26}$$

where $\alpha^\mu=\gamma^0\gamma^\mu=(1,\boldsymbol{\alpha})$ and $D_{\mu\nu}$ denotes the photon propagator. In the Feynman gauge, the propagator of a photon with the nonzero mass μ is

$$D_{\mu\nu}(\omega,\mathbf{x}-\mathbf{y}) = g_{\mu\nu}\frac{\exp(i\sqrt{\omega^2-\mu^2+i0}|\mathbf{x}-\mathbf{y}|)}{4\pi|\mathbf{x}-\mathbf{y}|}, \tag{27}$$

where it is assumed that $\mathrm{Im}\sqrt{\omega^2-\mu^2+i0}>0$. For the matrix elements of the operator $I(\omega)$ we will use the shorthand notation

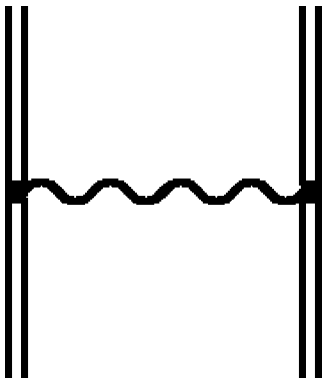

FIG. 1. The diagram of the one-photon exchange.

$$I_{ijkl}(\omega) = \langle ij|I(\omega)|kl\rangle. \tag{28}$$

B. One-photon exchange diagram

In order to illustrate how the method works, below we present the detailed derivation of the correction to the quasidegenerate energy levels $(1s2p_{1/2})_1$ and $(1s2p_{3/2})_1$ due to the one-photon exchange diagram (Fig. 1). While the corresponding evaluation is much less cumbersome than those for the second-order two-electron corrections, it demonstrates most essential features that are encountered in these cases. For simplicity, in the derivation below we will assume that the unperturbed energy of the initial state i differs from that of the final state k: $E_i^{(0)} \neq E_k^{(0)}$ (in the case under consideration it corresponds to $i \neq k$). However, all the final formulas can be shown to be valid also for the case $E_i^{(0)} = E_k^{(0)}$.

According to the Feynman rules [36,45] and the definition of $g(E)$, the contribution of the one-photon exchange diagram is

$$g_{ik}^{(1)}(E) = F_i F_k \left(\frac{i}{2\pi}\right)^2 \int_{-\infty}^{\infty} dp_1^0 dp'^0_1 \times \sum_P (-1)^P \frac{1}{(p'^0_1 - \varepsilon_{Pi_1} + i0)(E - p'^0_1 - \varepsilon_{Pi_2} + i0)} \times \frac{I_{Pi_1 Pi_2 k_1 k_2}(p'^0_1 - p_1^0)}{(p_1^0 - \varepsilon_{k_1} + i0)(E - p_1^0 - \varepsilon_{k_2} + i0)}. \tag{29}$$

Employing the identities

$$\frac{1}{(p'^0_1 - \varepsilon_{Pi_1} + i0)(E - p'^0_1 - \varepsilon_{Pi_2} + i0)} = \frac{1}{E - E_i^{(0)}} \left(\frac{1}{p'^0_1 - \varepsilon_{Pi_1} + i0} + \frac{1}{E - p'^0_1 - \varepsilon_{Pi_2} + i0} \right), \tag{30}$$

$$\frac{1}{(p_1^0 - \varepsilon_{k_1} + i0)(E - p_1^0 - \varepsilon_{k_2} + i0)} = \frac{1}{E - E_k^{(0)}} \left(\frac{1}{p_1^0 - \varepsilon_{k_1} + i0} + \frac{1}{E - p_1^0 - \varepsilon_{k_2} + i0} \right), \tag{31}$$

we obtain

$$K_{ik}^{(1)} = F_i F_k \frac{1}{2\pi i} \oint_\Gamma dE \frac{E}{(E - E_i^{(0)})(E - E_k^{(0)})} \left[\left(\frac{i}{2\pi}\right)^2 \int_{-\infty}^{\infty} dp_1^0 dp'^0_1 \sum_P (-1)^P \left(\frac{1}{p'^0_1 - \varepsilon_{Pi_1} + i0} + \frac{1}{E - p'^0_1 - \varepsilon_{Pi_2} + i0} \right) \times \left(\frac{1}{p_1^0 - \varepsilon_{k_1} + i0} + \frac{1}{E - p_1^0 - \varepsilon_{k_2} + i0} \right) I_{Pi_1 Pi_2 k_1 k_2}(p'^0_1 - p_1^0) \right]. \tag{32}$$

The expression in the square brackets is an analytical function of E inside the contour Γ, if the photon mass μ is chosen properly (see Refs. [35,45]). Carrying out the E integration by Cauchy's theorem and taking into account that

$$\left(\frac{i}{2\pi}\right)\left(\frac{1}{x + i0} + \frac{1}{-x + i0} \right) = \delta(x), \tag{33}$$

we obtain

$$K_{ik}^{(1)} = F_i F_k \left\{ \frac{i}{2\pi} \int_{-\infty}^{\infty} dp_1^0 \sum_P (-1)^P \frac{E_i^{(0)} I_{Pi_1 Pi_2 k_1 k_2}(\varepsilon_{Pi_1} - p_1^0)}{E_i^{(0)} - E_k^{(0)}} \left(\frac{1}{p_1^0 - \varepsilon_{k_1} + i0} + \frac{1}{E_i^{(0)} - p_1^0 - \varepsilon_{k_2} + i0} \right) + \frac{i}{2\pi} \times \int_{-\infty}^{\infty} dp'^0_1 \sum_P (-1)^P \frac{E_k^{(0)} I_{Pi_1 Pi_2 k_1 k_2}(p'^0_1 - \varepsilon_{k_1})}{E_k^{(0)} - E_i^{(0)}} \left(\frac{1}{p'^0_1 - \varepsilon_{Pi_1} + i0} + \frac{1}{E_k^{(0)} - p'^0_1 - \varepsilon_{Pi_2} + i0} \right) \right\}. \tag{34}$$

In the same way we find

$$P_{ik}^{(1)} = F_i F_k \left\{ \frac{i}{2\pi} \int_{-\infty}^{\infty} dp_1^0 \sum_P (-1)^P \frac{I_{Pi_1 Pi_2 k_1 k_2}(\varepsilon_{Pi_1} - p_1^0)}{E_i^{(0)} - E_k^{(0)}} \left(\frac{1}{p_1^0 - \varepsilon_{k_1} + i0} + \frac{1}{E_i^{(0)} - p_1^0 - \varepsilon_{k_2} + i0} \right) + \frac{i}{2\pi} \right.$$
$$\left. \times \int_{-\infty}^{\infty} dp'^0_1 \sum_P (-1)^P \frac{I_{Pi_1 Pi_2 k_1 k_2}(p'^0_1 - \varepsilon_{k_1})}{E_k^{(0)} - E_i^{(0)}} \left(\frac{1}{p'^0_1 - \varepsilon_{Pi_1} + i0} + \frac{1}{E_k^{(0)} - p'^0_1 - \varepsilon_{Pi_2} + i0} \right) \right\}. \tag{35}$$

Substituting Eqs. (34) and (35) into Eq. (17), we get

$$H_{ik}^{(1)} = F_i F_k \left\{ \frac{i}{4\pi} \int_{-\infty}^{\infty} dp_1^0 \sum_P (-1)^P I_{Pi_1 Pi_2 k_1 k_2}(\varepsilon_{Pi_1} - p_1^0) \left(\frac{1}{p_1^0 - \varepsilon_{k_1} + i0} + \frac{1}{E_i^{(0)} - p_1^0 - \varepsilon_{k_2} + i0} \right) + \frac{i}{4\pi} \right.$$
$$\left. \times \int_{-\infty}^{\infty} dp'^0_1 \sum_P (-1)^P I_{Pi_1 Pi_2 k_1 k_2}(p'^0_1 - \varepsilon_{k_1}) \left(\frac{1}{p'^0_1 - \varepsilon_{Pi_1} + i0} + \frac{1}{E_k^{(0)} - p'^0_1 - \varepsilon_{Pi_2} + i0} \right) \right\}. \tag{36}$$

Introducing the notations $\Delta_1 = \varepsilon_{Pi_1} - \varepsilon_{k_1}$ and $\Delta_2 = \varepsilon_{Pi_2} - \varepsilon_{k_2}$, we can rewrite Eq. (36) as follows:

$$H_{ik}^{(1)} = F_i F_k \frac{i}{8\pi} \int_{-\infty}^{\infty} d\omega \sum_P (-1)^P I_{Pi_1 Pi_2 k_1 k_2}(\omega) \left(\frac{1}{\omega + \Delta_1 + i0} + \frac{1}{\Delta_2 - \omega + i0} + \frac{1}{\omega + \Delta_2 + i0} + \frac{1}{\Delta_1 - \omega + i0} + \frac{1}{\omega - \Delta_1 + i0} \right.$$
$$\left. + \frac{1}{-\Delta_2 - \omega + i0} + \frac{1}{\omega - \Delta_2 + i0} + \frac{1}{-\Delta_1 - \omega + i0} \right) = F_i F_k \frac{1}{4} \int_{-\infty}^{\infty} d\omega \sum_P (-1)^P I_{Pi_1 Pi_2 k_1 k_2}(\omega) [\delta(\omega + \Delta_1) + \delta(\omega - \Delta_1)$$
$$+ \delta(\omega + \Delta_2) + \delta(\omega - \Delta_2)]. \tag{37}$$

Taking into account that $I(z) = I(-z)$, we finally obtain [35,47]

$$H_{ik}^{(1)} = F_i F_k \frac{1}{2} \sum_P (-1)^P [I_{Pi_1 Pi_2 k_1 k_2}(\Delta_1) + I_{Pi_1 Pi_2 k_1 k_2}(\Delta_2)]. \tag{38}$$

C. Two-photon exchange diagrams

The set of two-photon exchange diagrams is shown in Fig. 2. The first and the second graph are referred to as the ladder and the crossed diagram, respectively. The derivation of the general expressions for the two-photon exchange correction in the case of quasidegenerate levels is rather lengthy. However, it greatly resembles the corresponding derivation for the one-photon exchange correction presented above, on one hand, and that for the two-photon exchange diagram in case of a single level described in detail in Ref. [48], on the other hand. We thus present only the final formulas for the two-photon exchange contributions to the matrix elements of the operator $H^{(2)}$.

1. The ladder diagram

The contribution of the two-photon ladder diagram is conveniently divided into the *irreducible* and the *reducible* parts. The reducible contribution is defined as the part in which the total intermediate energy of the atom equals $E_1^{(0)}$ or $E_2^{(0)}$ and the irreducible part is the remainder. The operator $\hat{H}^{(2)}$ is defined by Eq. (18). The first three terms in the right-hand side of this equation contribute both to the irreducible and to the reducible parts. As to the others, it is natural to ascribe them to the reducible part.

The contribution of the irreducible part of $H_{ik}^{(2)}$ is defined as the self-adjoint part of the following matrix:

$$H_{ik}^{\mathrm{lad,ir}} = [K^{(2,\mathrm{ir})} - (1/2)P^{(2,\mathrm{ir})}K^{(0)} - (1/2)K^{(0)}P^{(2,\mathrm{ir})}]_{ik}. \tag{39}$$

The result is

$$H_{ik}^{\mathrm{lad,ir}} = F_i F_k \left\{ \frac{1}{4} [S_{ik}(E_i^{(0)},0,0) + S_{ik}(E_i^{(0)},0,\Delta) + S_{ik}(E_k^{(0)},0,0) \right.$$
$$+ S_{ik}(E_k^{(0)},-\Delta,0)] + \frac{i}{4\pi} \mathrm{P} \int_{-\infty}^{\infty} dx \frac{1}{x} [S_{ik}(E_i^{(0)},0,x)$$
$$- S_{ik}(E_i^{(0)},0,x+\Delta) + S_{ik}(E_k^{(0)},x,0)$$
$$\left. - S_{ik}(E_k^{(0)},x-\Delta,0)] \right\}, \tag{40}$$

where $\Delta = E_i^{(0)} - E_k^{(0)}$ and the matrix elements S_{ik} are defined by

$$S_{ik}(E,x,y) = \sum_P (-1)^P \frac{i}{2\pi}\int_{-\infty}^{\infty} d\omega \sum_{n_1 n_2}^{E_n^{(0)}\neq E_1^{(0)},E_2^{(0)}} \frac{I_{Pi_1Pi_2n_1n_2}(\varepsilon_{Pi_1}-\omega+x) I_{n_1n_2k_1k_2}(\varepsilon_{k_1}-\omega+y)}{[\omega-\varepsilon_{n_1}(1-i0)][E-\omega-\varepsilon_{n_2}(1-i0)]}. \tag{41}$$

The summation here runs over all n_1 and n_2 for which $E_n^{(0)} \neq E_1^{(0)}, E_2^{(0)}$, where $E_n^{(0)} \equiv \varepsilon_{n_1} + \varepsilon_{n_2}$ is the total intermediate energy of the atom. P in front of the integral in Eq. (40) denotes that the principal value of the integral (over x) must be taken.

We note that the part containing the integral over x in Eq. (40) vanishes identically in case of diagonal matrix elements ($i=k$). It also vanishes for single levels [48]. In case of off-diagonal matrix elements ($i \neq k$), the contribution of this part is of order $\alpha^2\Delta$ and it vanishes when $(E_i^{(0)} - E_k^{(0)}) \to 0$. As shown in Ref. [36], such terms contribute to the next order of perturbation theory and can, therefore, be disregarded in the present consideration. Expression (40) can be simplified even further by taking into account that

$$E_i^{(0)} = \overline{E}^{(0)} + O(\Delta), \quad E_k^{(0)} = \overline{E}^{(0)} + O(\Delta), \tag{42}$$

where $\overline{E}^{(0)} = (E_i^{(0)} + E_k^{(0)})/2$. We thus write $H_{ik}^{\mathrm{lad,ir}}$ simply as

$$H_{ik}^{\mathrm{lad,ir}} = F_i F_k S_{ik}(\overline{E}^{(0)},0,0) + O(\alpha^2\Delta) = F_i F_k \sum_P (-1)^P \frac{i}{2\pi}\int_{-\infty}^{\infty} d\omega \sum_{n_1 n_2}^{E_n^{(0)}\neq E_1^{(0)},E_2^{(0)}} \frac{I_{Pi_1Pi_2n_1n_2}(\varepsilon_{Pi_1}-\omega) I_{n_1n_2k_1k_2}(\varepsilon_{k_1}-\omega)}{[\omega-\varepsilon_{n_1}(1-i0)][\overline{E}^{(0)}-\omega-\varepsilon_{n_2}(1-i0)]} + O(\alpha^2\Delta). \tag{43}$$

The reducible contribution is induced by the self-adjoint part of the following operator

$$H^{\mathrm{lad,red}} = H^{\mathrm{lad,red},a} + H^{\mathrm{lad,red},b}, \tag{44}$$

where

$$H^{\mathrm{lad,red},a} = K^{(2,\mathrm{red})} - \frac{1}{2}P^{(2,\mathrm{red})}K^{(0)} - \frac{1}{2}K^{(0)}P^{(2,\mathrm{red})} \tag{45}$$

and

$$H^{\mathrm{lad,red},b} = -\frac{1}{2}P^{(1)}K^{(1)} - \frac{1}{2}K^{(1)}P^{(1)} + \frac{3}{8}P^{(1)}P^{(1)}K^{(0)} + \frac{3}{8}K^{(0)}P^{(1)}P^{(1)} + \frac{1}{4}P^{(1)}K^{(0)}P^{(1)}. \tag{46}$$

The result for the first part reads

$$H_{ik}^{\mathrm{lad,red},a} = F_i F_k \Bigg\{ -\frac{1}{2}[A_{ik}(0) + A_{ik}(\Delta) + B_{ik}(0) + B_{ik}(-\Delta) + C_{ik}] - \frac{1}{4}[D_{ik}(E_i^{(0)},0,0) + D_{ik}(E_i^{(0)},0,\Delta) + D_{ik}(E_k^{(0)},0,0) + D_{ik}(E_k^{(0)},-\Delta,0)] - \frac{i}{4\pi}\mathrm{P}\int_{-\infty}^{\infty} dx \frac{1}{x}[D_{ik}(E_i^{(0)},0,x) - D_{ik}(E_i^{(0)},0,x+\Delta) + D_{ik}(E_k^{(0)},x,0) - D_{ik}(E_k^{(0)},x-\Delta,0)] \Bigg\}, \tag{47}$$

where

$$A_{ik}(x) = \sum_P (-1)^P \frac{i}{2\pi} \sum_{n_1 n_2}^{E_n^{(0)}=E_1^{(0)},E_2^{(0)}} \int_{-\infty}^{\infty} d\omega \times \frac{I_{Pi_1Pi_2n_1n_2}(\omega-\varepsilon_{n_1}) I_{n_1n_2k_1k_2}(\varepsilon_{k_1}-\varepsilon_{n_1})}{(\omega-\varepsilon_{Pi_1}+E_i^{(0)}-E_n^{(0)}-i0)(\omega-\varepsilon_{Pi_1}+x-i0)}, \tag{48}$$

$$B_{ik}(x) = \sum_P (-1)^P \frac{i}{2\pi} \sum_{n_1 n_2}^{E_n^{(0)}=E_1^{(0)},E_2^{(0)}} \int_{-\infty}^{\infty} d\omega \times \frac{I_{Pi_1Pi_2n_1n_2}(\varepsilon_{Pi_1}-\varepsilon_{n_1}) I_{n_1n_2k_1k_2}(\omega-\varepsilon_{n_1})}{(\omega-\varepsilon_{k_1}+E_k^{(0)}-E_n^{(0)}-i0)(\omega-\varepsilon_{k_1}+x-i0)}, \tag{49}$$

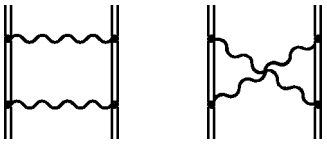

FIG. 2. The diagrams of the two-photon exchange.

$$C_{ik}=\sum_P(-1)^P\sum_{n_1n_2}^{E_n^{(0)}=E_1^{(0)},E_2^{(0)}}(E_i^{(0)}+E_k^{(0)}-2E_n^{(0)})\frac{i}{2\pi}\int_{-\infty}^{\infty}d\omega'\times\frac{I_{Pi_1Pi_2n_1n_2}(\omega'-\varepsilon_{n_1})}{(\omega'-\varepsilon_{Pi_1}-i0)(\omega'-\varepsilon_{Pi_1}+E_i^{(0)}-E_n^{(0)}-i0)}\frac{i}{2\pi}\times\int_{-\infty}^{\infty}d\omega\frac{I_{n_1n_2k_1k_2}(\omega-\varepsilon_{n_1})}{(\omega-\varepsilon_{k_1}-i0)(\omega-\varepsilon_{k_1}+E_k^{(0)}-E_n^{(0)}-i0)},\tag{50}$$

$$D_{ik}(E,x,y)=\sum_P(-1)^P\frac{i}{2\pi}\sum_{n_1n_2}^{E_n^{(0)}=E_1^{(0)},E_2^{(0)}}\int_{-\infty}^{\infty}d\omega\times\frac{I_{Pi_1Pi_2n_1n_2}(\varepsilon_{Pi_1}-\omega+x)I_{n_1n_2k_1k_2}(\varepsilon_{k_1}-\omega+y)}{(\omega-\varepsilon_{n_1}-i0)(\omega+\varepsilon_{n_2}-E-i0)}.\tag{51}$$

The part containing the integral over x in Eq. (47) represents a contribution of order $\alpha^2\Delta$. Again, we regard this contribution as belonging to the next order of perturbation theory and disregard it in the present investigation.

The second part of the reducible contribution is given by the matrix element of the operator (46). The result is obtained by taking into account that

$$K_{ik}^{(0)}=E_i^{(0)}\delta_{ik},\quad P_{ik}^{(0)}=\delta_{ik},\tag{52}$$

$$K_{ik}^{(1)}=F_iF_k\sum_P(-1)^P\left\{\frac{1}{2}[I_{Pi_1Pi_2k_1k_2}(\Delta_1)+I_{Pi_1Pi_2k_1k_2}(\Delta_2)]-\frac{(E_i^{(0)}+E_k^{(0)})}{2}\frac{i}{2\pi}\int_{-\infty}^{\infty}d\omega\,I_{Pi_1Pi_2k_1k_2}(\omega)\times\left[\frac{1}{(\omega+\Delta_1-i0)(\omega-\Delta_2-i0)}+\frac{1}{(\omega+\Delta_2-i0)(\omega-\Delta_1-i0)}\right]\right\},\tag{53}$$

and

$$P_{ik}^{(1)}=-F_iF_k\sum_P(-1)^P\frac{i}{2\pi}\int_{-\infty}^{\infty}d\omega\,I_{Pi_1Pi_2k_1k_2}(\omega)\times\left[\frac{1}{(\omega+\Delta_1-i0)(\omega-\Delta_2-i0)}+\frac{1}{(\omega+\Delta_2-i0)(\omega-\Delta_1-i0)}\right].\tag{54}$$

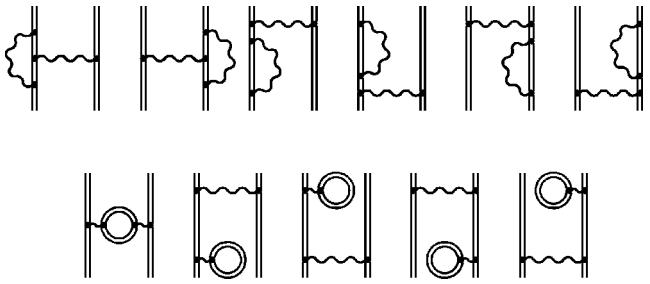

FIG. 3. Self-energy screening and vacuum-polarization screening diagrams.

The total result for the reducible part can be simplified by using Eq. (42) and disregarding terms that contribute to the next order of perturbation theory. One can show that in this case the A's, B's, and C's in Eq. (47) are canceled completely by the $H^{\mathrm{lad,red},b}$ term. The result is just

$$H_{ik}^{\mathrm{lad,red}}=-F_iF_kD_{ik}(\overline{E}^{(0)},0,0)+O(\alpha^2\Delta)=-F_iF_k\sum_P(-1)^P\sum_{n_1n_2}^{E_n^{(0)}=E_1^{(0)},E_2^{(0)}}\frac{i}{2\pi}\times\int_{-\infty}^{\infty}d\omega\frac{I_{Pi_1Pi_2n_1n_2}(\varepsilon_{Pi_1}-\omega)I_{n_1n_2k_1k_2}(\varepsilon_{k_1}-\omega)}{(\omega-\varepsilon_{n_1}-i0)(\omega+\varepsilon_{n_2}-\overline{E}^{(0)}-i0)}+O(\alpha^2\Delta).\tag{55}$$

2. The crossed diagram

The contribution of the crossed diagram is induced by the self-adjoint part of the operator

$$H^{\mathrm{cr}}=K^{(2)}-(1/2)P^{(2)}K^{(0)}-(1/2)K^{(0)}P^{(2)}.\tag{56}$$

The corresponding result reads

$$H_{ik}^{\mathrm{cr}}=F_iF_k\left\{\frac{1}{4}[T_{ik}(E_i^{(0)},0,0)+T_{ik}(E_i^{(0)},0,\Delta)+T_{ik}(E_k^{(0)},0,0)+T_{ik}(E_k^{(0)},-\Delta,0)]+\frac{i}{4\pi}\mathrm{P}\int_{-\infty}^{\infty}dx\frac{1}{x}[T_{ik}(E_i^{(0)},0,x)-T_{ik}(E_i^{(0)},0,x+\Delta)+T_{ik}(E_k^{(0)},x,0)-T_{ik}(E_k^{(0)},x-\Delta,0)]\right\},\tag{57}$$

where

$$T_{ik}(E,x,y)=\sum_P(-1)^P\sum_{n_1n_2}\frac{i}{2\pi}\int_{-\infty}^{\infty}d\omega\frac{I_{Pi_1n_2n_1k_2}(\varepsilon_{Pi_1}-\omega+x)I_{n_1Pi_2k_1n_2}(\varepsilon_{k_1}-\omega+y)}{[\omega-\varepsilon_{n_1}(1-i0)][E-\varepsilon_{Pi_1}-\varepsilon_{k_1}-x-y+\omega-\varepsilon_{n_2}(1-i0)]}.\tag{58}$$

The expression (57) can be simplified in the same way as the previous contributions, with the result

$$H_{ik}^{\rm cr} = F_i F_k T_{ik}(\overline{E}^{(0)},0,0) + O(\alpha^2\Delta) = F_i F_k \sum_P (-1)^P \sum_{n_1 n_2} \frac{i}{2\pi}\int_{-\infty}^{\infty} d\omega \frac{I_{P i_1 n_2 n_1 k_2}(\varepsilon_{P i_1}-\omega) I_{n_1 P i_2 k_1 n_2}(\varepsilon_{k_1}-\omega)}{[\omega-\varepsilon_{n_1}(1-i0)][\overline{E}^{(0)}-\varepsilon_{P i_1}-\varepsilon_{k_1}+\omega-\varepsilon_{n_2}(1-i0)]} + O(\alpha^2\Delta). \tag{59}$$

D. Screened self-energy correction

The set of Feynman diagrams representing the screened self-energy correction is shown in Fig. 3. Formal expressions for this correction in the case of quasidegenerate states were obtained previously in Ref. [49] by the TTGF method. Here we present only the final expressions for this correction.

The contribution of the vertex diagrams is given by

$$H_{ik}^{\rm ver} = F_i F_k \sum_P (-1)^P \frac{i}{2\pi}\int_{-\infty}^{\infty} d\omega \sum_{n_1 n_2} \left\{ \frac{I_{n_1 P i_2 n_2 k_2}(\Delta_1) I_{P i_1 n_2 n_1 k_1}(\omega)}{[\varepsilon_{P i_1}-\omega-\varepsilon_{n_1}(1-i0)][\varepsilon_{k_1}-\omega-\varepsilon_{n_2}(1-i0)]} + \frac{I_{P i_1 n_1 k_1 n_2}(\Delta_2) I_{P i_2 n_2 n_1 k_2}(\omega)}{[\varepsilon_{P i_2}-\omega-\varepsilon_{n_1}(1-i0)][\varepsilon_{k_2}-\omega-\varepsilon_{n_2}(1-i0)]} \right\} + O(\alpha^2\Delta), \tag{60}$$

where $\Delta_1=\varepsilon_{P i_1}-\varepsilon_{k_1}$ and $\Delta_2=\varepsilon_{P i_2}-\varepsilon_{k_2}$.

The contribution of the remaining diagrams is conveniently separated into the irreducible and reducible parts. The irreducible contribution is given by

$$\begin{aligned} H_{ik}^{\rm se,ir} = F_i F_k \sum_P (-1)^P \Bigg\{ & \sum_{n\neq k_1} \frac{I_{P i_1 P i_2 n k_2}(\Delta_1)}{\varepsilon_{k_1}-\varepsilon_n}\langle n|\Sigma(\varepsilon_{k_1})|k_1\rangle \\ & + \sum_{n\neq k_2} \frac{I_{P i_1 P i_2 k_1 n}(\Delta_2)}{\varepsilon_{k_2}-\varepsilon_n}\langle n|\Sigma(\varepsilon_{k_2})|k_2\rangle \\ & + \sum_{n\neq P i_1} \langle P i_1|\Sigma(\varepsilon_{P i_1})|n\rangle \frac{I_{n P i_2 k_1 k_2}(\Delta_1)}{\varepsilon_{P i_1}-\varepsilon_n} \\ & + \sum_{n\neq P i_2} \langle P i_2|\Sigma(\varepsilon_{P i_2})|n\rangle \frac{I_{P i_1 n k_1 k_2}(\Delta_2)}{\varepsilon_{P i_2}-\varepsilon_n} \Bigg\} + O(\alpha^2\Delta), \end{aligned} \tag{61}$$

where $\Sigma(\varepsilon)$ is the self-energy operator defined by its matrix elements,

$$\langle a|\Sigma(\varepsilon)|b\rangle = \frac{i}{2\pi}\int_{-\infty}^{\infty} d\omega \sum_n \frac{\langle an|I(\omega)|nb\rangle}{\varepsilon-\omega-\varepsilon_n(1-i0)}. \tag{62}$$

The result for the reducible contribution reads

$$\begin{aligned} H_{ik}^{\rm se,red} = F_i F_k \frac{1}{2}\sum_P (-1)^P \{ & I_{P i_1 P i_2 k_1 k_2}(\Delta_1)[\langle P i_1|\Sigma'(\varepsilon_{P i_1})|P i_1\rangle \\ & + \langle k_1|\Sigma'(\varepsilon_{k_1})|k_1\rangle] + I_{P i_1 P i_2 k_1 k_2}(\Delta_2)[\langle P i_2|\Sigma'(\varepsilon_{P i_2})|P i_2\rangle \\ & + \langle k_2|\Sigma'(\varepsilon_{k_2})|k_2\rangle] + I'_{P i_1 P i_2 k_1 k_2}(\Delta_1)[\langle P i_1|\Sigma(\varepsilon_{P i_1})|P i_1\rangle \\ & - \langle k_1|\Sigma(\varepsilon_{k_1})|k_1\rangle] + I'_{P i_1 P i_2 k_1 k_2}(\Delta_2)[\langle P i_2|\Sigma(\varepsilon_{P i_2})|P i_2\rangle \\ & - \langle k_2|\Sigma(\varepsilon_{k_2})|k_2\rangle]\} + O(\alpha^2\Delta), \end{aligned} \tag{63}$$

where $I'(\omega)\equiv\partial I(\omega)/\partial\omega$ and $\Sigma'(\omega)\equiv\partial\Sigma(\omega)/\partial\omega$.

E. Screened vacuum-polarization correction

The derivation of formal expressions for the screened vacuum-polarization correction in case of quasidegenerate states was described in our previous work [39]. For completeness, we present here the final expressions for this correction; the corresponding set of Feynman diagrams is shown in Fig. 3.

The expression for the contribution of the diagram with the vacuum-polarization loop inserted into the photon propagator can be obtained from the formula for the one-photon exchange (38) by replacing the operator of the electron-electron interaction $I(\varepsilon)$ by the modified interaction

$$\begin{aligned} U_{\rm VP}^{\rm ph}(\varepsilon,\mathbf{x},\mathbf{y}) = \frac{\alpha^2}{2\pi i}\int_{-\infty}^{\infty} d\omega \int d\mathbf{z}_1 d\mathbf{z}_2 \frac{\alpha_\mu \exp(i|\varepsilon||\mathbf{x}-\mathbf{z}_1|)}{|\mathbf{x}-\mathbf{z}_1|} \\ \times \frac{\alpha_\nu \exp(i|\varepsilon||\mathbf{y}-\mathbf{z}_2|)}{|\mathbf{y}-\mathbf{z}_2|} {\rm Tr}[\alpha^\mu G(\omega-\varepsilon/2,\mathbf{z}_1,\mathbf{z}_2) \\ \times \alpha^\nu G(\omega+\varepsilon/2,\mathbf{z}_2,\mathbf{z}_1)], \end{aligned} \tag{64}$$

where $G(\omega,\mathbf{x},\mathbf{y})=\Sigma_n \psi_n(\mathbf{x})\psi_n^\dagger(\mathbf{y})/[\omega-\varepsilon_n(1-i0)]$ is the Dirac-Coulomb Green's function. The corresponding contribution to $H_{ik}^{(2)}$ is

$$\begin{aligned} H_{ik}^{\rm VP,ph} = F_i F_k \frac{1}{2}\sum_P (-1)^P [& \langle P i_1 P i_2|U_{\rm VP}^{\rm ph}(\Delta_1)|k_1 k_2\rangle \\ & + \langle P i_1 P i_2|U_{\rm VP}^{\rm ph}(\Delta_2)|k_1 k_2\rangle], \end{aligned} \tag{65}$$

where $\Delta_1=\varepsilon_{P i_1}-\varepsilon_{k_1}$ and $\Delta_2=\varepsilon_{P i_2}-\varepsilon_{k_2}$.

To the order under consideration, expressions for the remaining diagrams can be obtained from the one-photon exchange correction by perturbing the wave functions and the binding energies by an additional vacuum-polarization interaction. The result is

$$H_{ik}^{\mathrm{VP,WF}} + H_{ik}^{\mathrm{VP,BE}} = F_i F_k \frac{1}{2}\sum_P (-1)^P \{\langle \delta P i_1 P i_2 | [I(\Delta_1) + I(\Delta_2)] | k_1 k_2\rangle + \langle P i_1 \delta P i_2 | [I(\Delta_1) + I(\Delta_2)] | k_1 k_2\rangle + \langle P i_1 P i_2 | [I(\Delta_1) + I(\Delta_2)] | \delta k_1 k_2\rangle + \langle P i_1 P i_2 | [I(\Delta_1) + I(\Delta_2)] | k_1 \delta k_2\rangle + (\delta\varepsilon_{P i_1} - \delta\varepsilon_{k_1})\langle P i_1 P i_2 | I'(\Delta_1) | k_1 k_2\rangle + (\delta\varepsilon_{P i_2} - \delta\varepsilon_{k_2}) \times \langle P i_1 P i_2 | I'(\Delta_2) | k_1 k_2\rangle\}, \quad (66)$$

where δi and δk refer to the first-order corrections to the corresponding wave function,

$$|\delta i\rangle = \sum_n^{\varepsilon_n \neq \varepsilon_i} \frac{|n\rangle\langle n|U_{\mathrm{VP}}|i\rangle}{\varepsilon_i - \varepsilon_n}, \quad (67)$$

$\delta\varepsilon_i$ is the correction to the energy, $\delta\varepsilon_i = \langle i|U_{\mathrm{VP}}|i\rangle$, and

$$U_{\mathrm{VP}}(\mathbf{x}) = \frac{\alpha}{2\pi i}\int_{-\infty}^{\infty} d\omega \int d\mathbf{y} \frac{1}{|\mathbf{x}-\mathbf{y}|} \mathrm{Tr}[G(\omega,\mathbf{y},\mathbf{y})] \quad (68)$$

is the vacuum-polarization potential.

As discussed previously in Ref. [36], a direct derivation based on the TTGF method yields a result that differs from Eq. (66) by terms of order $(\alpha^2\Delta)$, which can be disregarded as long as we are not interested in higher orders of perturbation theory (see Ref. [36] for a detailed discussion).

II. NUMERICAL EVALUATION AND RESULTS

An important difference of the present investigation from the previous studies of QED effects in high-Z ions is that it involves QED corrections for *quasidegenerate* configurations, namely, $(1s2p_{1/2})_1$ and $(1s2p_{3/2})_1$. While the derivation of basic expressions in this case is more difficult than for a single state, the final expressions for the diagonal matrix elements turn out to be very similar to those for the single-level case. We can, therefore, adopt a code developed for single-level calculations for the diagonal matrix elements of the operator H. For an evaluation of the off-diagonal matrix elements, a generalization of the code is needed.

The numerical procedure employed in the present calculation of the two-photon exchange correction is based on that presented in detail in our previous investigations for Li-like ions [32,50]. Apart from the angular reduction that is performed by using the standard angular-momentum technique, the evaluation is rather similar to that for Li-like ions. The calculation was carried out employing the Fermi model for the nuclear-charge distribution, with the nuclear charge radii specified in Ref. [32]. The numerical uncertainty of the results is expected to be 1×10^{-4} eV in all cases except for the off-diagonal matrix element, for which the uncertainty is 1×10^{-4} eV for $Z\leqslant 50$, 2×10^{-4} eV for $Z\leqslant 80$, and 4×10^{-4} eV otherwise. As a check of the numerical procedure, we performed the evaluation in two different gauges, the Feynman and the Coulomb ones. The two-photon exchange corrections (for mixing configurations, individual matrix elements) were found to be gauge invariant well within the uncertainty specified.

The results of our numerical calculation of the two-photon exchange correction for $n=1$ and 2 states of He-like ions are presented in Table I. The values listed represent corrections to the energy in the case of single levels and contributions to the matrix elements H_{ik} for the quasidegenerate states. The energy levels for the $(1s2p_{1/2})_1$ and $(1s2p_{3/2})_1$ states are obtained by diagonalizing the 2×2 matrix H containing all relevant corrections. In Table I, we present also a comparison of our numerical values with the results of the previous calculations of this correction for various states of He-like ions [25,38,40–43]. The comparison indicates that calculations by different groups are generally in agreement with each other. However, there exist also certain deviations between different calculations, notably with those by Andreev *et al.* [41,42]. Regarding the comparison of the present results and the ones of Ref. [38] for the mixing states, we would like to stress that, generally speaking, results of different methods for individual matrix elements could be different, since the matrix H can differ by a unitary transformation. We observe, however, that in our case the results for the individual matrix elements agree with those of Ref. [38] approximately at the same level as for the single states.

The calculation of the screened self-energy correction for $n=2$ states of He-like ions resembles that for Li-like ions described in our previous work [31]. A more difficult angular structure of the initial-state wave functions for He-like ions makes final expressions more lengthy and their numerical evaluation more time consuming. Significant complications appear in performing angular integrations in momentum space for the vertex part with free-electron propagators. To handle them, we developed a generalization of the angular-integration procedure described in Ref. [31] to arbitrary states, using our experience in calculating similar angular integrals for the two-loop self-energy diagrams [51]. The actual calculation was carried out employing the spherical-shell model for the nuclear-charge distribution. Our numerical results for the screened self-energy correction for $n=1$ and 2 states of He-like ions are presented in Table II in terms of the dimensionless function $F(\alpha Z)$ defined as

$$\Delta E = \alpha^2(\alpha Z)^3 F(\alpha Z). \quad (69)$$

The values listed in the table represent corrections to the energy in case of single levels and contributions to the matrix elements H_{ik} for the quasidegenerate states.

TABLE I. The two-photon exchange correction for $n=1$ and 2 states of He-like ions, in eV. For mixing configurations, $(1s2p_{1/2})_1$ and $(1s2p_{3/2})_1$ stand for the diagonal matrix elements of the operator H [see Eqs. (9) and (10)], whereas "off-diag." labels the off-diagonal matrix elements.

Z	$(1s1s)_0$	$(1s2s)_0$	$(1s2s)_1$	$(1s2p_{1/2})_0$	$(1s2p_{1/2})_1$	$(1s2p_{3/2})_1$	$(1s2p_{3/2})_2$	off-diag.
12	−4.4186	−3.1741	−1.2991	−2.0506	−2.7789	−3.5332	−1.9964	−1.0711
14	−4.4645	−3.1952	−1.3024	−2.0741	−2.7899	−3.5413	−2.0000	−1.0686
		−3.19541[b]	−1.30240[b]					
16	−4.5173	−3.2196	−1.3062	−2.1015	−2.8027	−3.5507	−2.0041	−1.0658
18	−4.5770	−3.2473	−1.3106	−2.1328	−2.8173	−3.5613	−2.0088	−1.0626
		−3.24753[b]	−1.31057[b]		−2.8168[e]	−3.5603[e]		−1.0618[e]
20	−4.6435	−3.2784	−1.3154	−2.1682	−2.8337	−3.5733	−2.0141	−1.0589
	−4.6447[a]							
28	−4.9784	−3.4378	−1.3405	−2.3532	−2.9182	−3.6340	−2.0405	−1.0406
30	−5.0795	−3.4868	−1.3483	−2.4111	−2.9443	−3.6525	−2.0484	−1.0350
	−5.0812[a]	−3.48716[b]	−1.34827[b]	−2.41112[d]	−2.9439[e]	−3.6506[e]	−2.04834[d]	−1.0350[e]
		−3.473[c]	−1.348[c]					
			−1.34833[d]					
32	−5.1877	−3.5396	−1.3566	−2.4741	−2.9725	−3.6724	−2.0568	−1.0291
40	−5.6924	−3.7919	−1.3961	−2.7817	−3.1072	−3.7658	−2.0956	−1.0015
	−5.6945[b]		−1.39621[d]	−2.78172[d]	−3.1082[e]	−3.7641[e]	−2.09545[b]	−1.0008[e]
47	−6.2332	−4.0719	−1.4395	−3.1351	−3.2575	−3.8668	−2.1358	−0.9724
50	−6.4951	−4.2110	−1.4609	−3.3148	−3.3323	−3.9159	−2.1548	−0.9586
	−6.4975[a]		−1.46120[d]	−3.31489[d]	−3.333[e]	−3.915[e]	−2.15465[d]	−0.955[e]
54	−6.8742	−4.4162	−1.4923	−3.5848	−3.4429	−3.9871	−2.1816	−0.9387
60	−7.5114	−4.7714	−1.5459	−4.0642	−3.6348	−4.1066	−2.2251	−0.9064
	−7.5142[a]	−4.77215[b]	−1.54587[b]	−4.068[c]	−3.635[e]	−4.105[e]	−2.22510[d]	−0.893[e]
		−4.781[c]	−1.542[c]	−4.06446[d]				
			−1.54558[d]					
66	−8.2393	−5.1924	−1.6082	−4.6505	−3.8632	−4.2426	−2.2724	−0.8708
		−5.194[c]	−1.605[c]	−4.670[c]				
70	−8.7812	−5.5159	−1.6552	−5.1131	−4.0394	−4.3430	−2.3060	−0.8453
	−8.7847[a]	−5.515[c]	−1.648[c]	−5.117[c]	−4.038[e]	−4.339[e]	−2.30573[d]	−0.801[e]
			−1.65478[d]	−5.11403[d]				
74	−9.3739	−5.8794	−1.7073	−5.6441	−4.2381	−4.4517	−2.3412	−0.8184
79	−10.1957	−6.3996	−1.7803	−6.4220	−4.5238	−4.5999	−2.3877	−0.7826
80	−10.3719	−6.5135	−1.7961	−6.5950	−4.5866	−4.6312	−2.3974	−0.7752
	−10.375[a]	−6.504[c]	−1.789[c]	−6.598[c]	−4.585[e]	−4.628[e]	−2.39806[d]	−0.771[e]
			−1.79562[d]	−6.59593[d]				
82	−10.7375	−6.7524	−1.8289	−6.9607	−4.7185	−4.6957	−2.4170	−0.7601
83	−10.9271	−6.8776	−1.8460	−7.1540	−4.7877	−4.7288	−2.4270	−0.7524
90	−12.3979	−7.8792	−1.9790	−8.7331	−5.3458	−4.9780	−2.5005	−0.6957
	−12.403[a]							
92	−12.8714	−8.2122	−2.0221	−9.2701	−5.5329	−5.0550	−2.5228	−0.6787
		−8.21306[b]	−2.02199[b]	−9.274[c]	−5.531[e]	−5.053[e]	−2.52228[d]	−0.683[d]
		−8.184[c]	−2.018[c]	−9.27598[d]				
			−2.02034[d]					
100	−15.0772	−9.8239	−2.2223	−11.9330	−6.4484	−5.3900	−2.6191	−0.6058
	−15.0805[a]							

[a]Blundell *et al.* [25].
[b]Åsen *et al.* [43].
[c]Andreev *et al.* [41,42].
[d]Mohr and Sapirstein [40].
[e]Andreev *et al.* [38].

TABLE II. Screened self-energy correction for $n=1$ and 2 states of He-like ions, in units of $F(\alpha Z)$. In case of mixing configurations, contributions to the matrix elements H_{ik} are given; labeling is as in Table I.

Z	$(1s1s)_0$	$(1s2s)_0$	$(1s2s)_1$	$(1s2p_{1/2})_0$	$(1s2p_{1/2})_1$	$(1s2p_{3/2})_1$	$(1s2p_{3/2})_2$	off-diag.
12	−2.2139(8)	−0.4841(5)	−0.3031(5)	−0.0917(6)	−0.0691(6)	−0.0556(7)	−0.1350(7)	0.0533(2)
14	−2.0543(6)	−0.4519(4)	−0.2821(4)	−0.0845(5)	−0.0646(5)	−0.0537(6)	−0.1266(6)	0.0490(1)
16	−1.9217(3)	−0.4248(3)	−0.2646(3)	−0.0783(4)	−0.0605(4)	−0.0517(4)	−0.1197(4)	0.04559(5)
18	−1.8097(3)	−0.4021(3)	−0.2496(3)	−0.0733(2)	−0.0571(2)	−0.0501(2)	−0.1137(2)	0.04266(3)
20	−1.7137(3)	−0.3828(3)	−0.2368(3)	−0.0693(1)	−0.0544(1)	−0.0488(2)	−0.1086(2)	0.04013(3)
30	−1.3888(2)	−0.3194(2)	−0.1930(2)	−0.0581(1)	−0.0470(1)	−0.0452(2)	−0.0913(2)	0.03146(2)
40	−1.2112(1)	−0.2879(1)	−0.1685(1)	−0.05588(7)	−0.04542(7)	−0.0442(1)	−0.0817(1)	0.02639(2)
50	−1.1134(1)	−0.2746(1)	−0.1547(1)	−0.05963(8)	−0.04784(8)	−0.0449(1)	−0.0761(1)	0.02312(2)
60	−1.0679(1)	−0.2744(1)	−0.1478(1)	−0.06871(6)	−0.05371(6)	−0.0465(1)	−0.0729(1)	0.02087(1)
70	−1.06281(5)	−0.28559(5)	−0.14670(5)	−0.08394(5)	−0.06349(5)	−0.04896(7)	−0.07136(7)	0.019257(8)
80	−1.09510(3)	−0.30916(3)	−0.15096(3)	−0.10779(2)	−0.07864(2)	−0.05197(7)	−0.07091(7)	0.018047(6)
83	−1.11237(2)	−0.31903(2)	−0.15336(2)	−0.11728(2)	−0.08463(2)	−0.05294(7)	−0.07094(7)	0.017741(5)
90	−1.16760(2)	−0.34804(2)	−0.16122(2)	−0.14526(1)	−0.10222(1)	−0.05530(7)	−0.07130(7)	0.017104(3)
92	−1.18776(2)	−0.35814(2)	−0.16413(2)	−0.15515(1)	−0.10841(1)	−0.05600(7)	−0.07148(7)	0.016939(3)
100	−1.29293(2)	−0.40917(2)	−0.17942(2)	−0.20688(3)	−0.14073(3)	−0.05881(7)	−0.07250(7)	0.016343(3)

In case of the ground state of He-like ions, the self-energy correction was evaluated previously by Persson *et al.* [27], by us [29], and by Sunnergren [52]. In the present work, we recalculated this correction using the present code and found an excellent agreement with our previous results and with those by Sunnergren. A small deviation of the present result for $Z=90$ from the old one is due to a more recent value for the nuclear charge radius used in this work.

We note that the values presented in Table II for $n=2$ states of He-like ions can also be used for determining the screened self-energy correction due to the interaction of the valence electron and the $(1s)^2$ shell in Li-like ions. Indeed, by using elementary angular-summation rules, we obtain

$$(2j_v+1)\Delta E_v^{\mathrm{Li}} = \sum_J (2J+1)\Delta E_{v,J}^{\mathrm{He}}, \tag{70}$$

where ΔE_v^{Li} denotes the screened self-energy correction in a Li-like ion due to the interaction of the electron in the state v and the $(1s)^2$ shell, $\Delta E_{v,J}^{\mathrm{He}}$ is the screened self-energy correction in a He-like ion for the $(1s\ v)_J$ configuration (in the case of mixing configurations, a diagonal matrix element should be taken), and j_v is the total angular momentum of the v electron. By employing the identity (70), we check that our numerical results for He-like ions are in a very good agreement with our previous calculations for Li-like ions [31].

Our calculations of the screened self-energy and two-photon exchange corrections, combined with the results for the screened vacuum-polarization from Ref. [39] (with the off-diagonal matrix elements corrected in this paper; see below), complete the evaluation of the QED correction to first order in $1/Z$ and to all orders in αZ for $n=2$ states of He-like ions. As is known, the αZ expansion of two-electron QED effects starts with $\alpha^2(\alpha Z)^3$. The two-photon exchange correction contains also contributions of previous orders in αZ that can be derived from the Breit equation. We separate the "pure" QED part of the two-photon exchange contribution ($\Delta E_{2\mathrm{ph}}^{\mathrm{QED}}$) as

$$\Delta E_{2\mathrm{ph}} = \alpha^2[a_0 + (\alpha Z)^2 a_2] + \Delta E_{2\mathrm{ph}}^{\mathrm{QED}}, \tag{71}$$

where $\Delta E_{2\mathrm{ph}}$ is the total two-photon exchange correction and $\Delta E_{2\mathrm{ph}}^{\mathrm{QED}}$ contributes to order $\alpha^2(\alpha Z)^3$ and higher. In order to extract numerical values for $\Delta E_{2\mathrm{ph}}^{\mathrm{QED}}$ from our results for $\Delta E_{2\mathrm{ph}}$ without losses in accuracy, accurate values for the coefficients a_0 and a_2 are needed. We calculate them by fitting our results for the two-photon exchange correction obtained within many-body perturbation theory. A large number of fitting points and inclusion of fraction values for the nuclear charge number (up to $Z=0.1$) allowed us to achieve better accuracy than in previous calculations of similar coefficients (e.g., Refs. [18,53,54]). The numerical results for the coefficients a_0 and a_2 for all states under consideration are tabulated in the second and in the third columns of Table III, respectively.

In Table IV we collect all two-electron QED contributions for $n=1$ and 2 states of He-like ions. The screened self-energy and two-photon exchange corrections are calculated in the present work; in the table they are labeled as "Scr.SE" and "2-ph.exch.," respectively. The screened vacuum-polarization correction was first evaluated in our previous investigation [39]. In the present work, we correct an error made in Ref. [39] for the off-diagonal matrix element and extend our calculation to the region $10<Z<20$. Numerical values for the screened vacuum-polarization correction are listed in Table IV under the entry "Scr.VP."

Our results for the two-electron QED correction calculated to all orders in αZ can be compared with the results obtained within the αZ expansion, which reads [1,2]

TABLE III. Coefficients of the αZ expansion of the second-order two-electron contribution to the energy levels of He-like ions. In case of mixing configurations, contributions to the matrix elements H_{ik} are given; labeling is as in Table I.

	$(\alpha Z)^0$	$(\alpha Z)^2$	$(\alpha Z)^3 \ln \alpha Z$	$(\alpha Z)^3$	$(\alpha Z)^4 \ln \alpha Z$	$(\alpha Z)^4$
$(1s1s)_0$	−0.157662	−0.6302	1.3191	1.6588	0.75(15)	−2.41(40)
$(1s2s)_0$	−0.114509	−0.2807	0.2755	0.3255	0.11(2)	−0.81(5)
$(1s2s)_1$	−0.047409	−0.0428	0.1795	0.1911	0.056(11)	−0.40(3)
$(1s2p_{1/2})_0$	−0.072999	−0.3035	0.0730	0.1063	0	−0.64(2)
$(1s2p_{1/2})_1$	−0.101008	−0.1444	0.0465	0.0578	0	−0.22(1)
$(1s2p_{3/2})_1$	−0.129018	−0.1075	0.0201	0.0058	0	−0.10
$(1s2p_{3/2})_2$	−0.072999	−0.0473	0.0730	0.0595	0.01(1)	−0.14(2)
off-diag.	−0.039611	0.0319	−0.0374	−0.0432	−0.01(1)	0.08(4)

$$\Delta E_{2\mathrm{el}}^{\mathrm{QED}} = \alpha^2(\alpha Z)^3[a_{31}\ln \alpha Z + a_{30} + (\alpha Z)G_{2\mathrm{el}}^{\mathrm{ho}}(\alpha Z)], \tag{72}$$

where the function $G_{2\mathrm{el}}^{\mathrm{ho}}(\alpha Z)$ is the higher-order remainder that is not known analytically at present. We obtain numerical values for the coefficients a_{31} and a_{30} by using formulas from Ref. [1] and numerical results for the two-electron Bethe logarithms [55] and for the $1/Z$-expansion coefficients of expectation values of various operators [18,56]. The only coefficient whose numerical value was not available in the literature was the anomalous magnetic moment correction for the off-diagonal matrix element. This is the first-order $1/Z$-expansion term of the matrix element of the operator $\alpha/\pi(H'''_3+H'''_5)$ [see Eqs. (27) and (28) of Ref. [56]]. The result of our calculation of this correction (denoted in Ref. [18] as ΔE_{anom}) for the off-diagonal term in the *LS* coupling reads

$$\Delta E_{\mathrm{anom}}^{LS}(\text{off diag}) = \alpha^2(\alpha Z)^3 0.010\,110. \tag{73}$$

Numerical values for the coefficients a_{31} and a_{30} for all states under consideration are listed in the third and in the fourth columns of Table III, respectively.

In Fig. 4, we plot our numerical results together with the contribution of the first two terms of the αZ expansion (dashed line). In addition, we also plot the two-electron QED contribution, as evaluated by Drake [18] (dotted line). It was obtained according Eqs. (2)–(9) of Ref. [18], keeping the contribution of first order in $1/Z$ only. [We note that Eq. (8) of Ref. [18] contains a misprint; its right-hand side should be multiplied by *Z*.] Expressions obtained in this way are exact to the leading order $\alpha^2(\alpha Z)^3$. They also contain some higher-order contributions, due to all-order results for the one-electron QED correction employed for the evaluation of the $E_{L,1}$ term [Eq. (2) of Ref. [18]]. We observe a good agreement of our results with the previously known contributions and conclude that Drake's values fall much closer to our all-order results than the pure αZ-expansion contribution.

For mixing states $(1s2p_{1/2})_1$ and $(1s2p_{3/2})_1$, Fig. 4 presents a comparison for individual diagonal and off-diagonal matrix elements. It should be mentioned that, generally speaking, comparison of different methods should be performed for the physical energies obtained after the diagonalization of the total matrix and not for the individual matrix elements, since matrices with the same eigenvalues can differ by a unitary transformation. We see from Fig. 4, however, that our results are in a good agreement with the αZ-expansion contributions also for the individual matrix elements.

An agreement found with the leading term of the αZ expansion offers us a possibility to obtain the next-to-leading contribution, which is not known analytically at present, and in this way to extend the results of our calculations to lower values of *Z*. We thus isolate the higher-order remainder $G_{2\mathrm{el}}^{\mathrm{ho}}(\alpha Z)$ [see Eq. (72)] from our numerical data and fit it to the form

$$G_{2\mathrm{el}}^{\mathrm{ho}}(\alpha Z) = a_{41}\ln \alpha Z + a_{40} + (\alpha Z)(\cdots). \tag{74}$$

Fitted values for the coefficients a_{41} and a_{40} are presented in the last two columns of Table III. It should be stressed that these coefficients were obtained in the *jj*-coupling scheme with the wave functions defined in case of mixing states by Eqs. (1) and (2).

There is a way to test the self-consistency of the numerical results for individual matrix elements, and to check each two-electron QED contribution separately. We note that, in the *LS* coupling, the only contribution to the off-diagonal matrix element to order $\alpha^2(\alpha Z)^3$ is that of the anomalous magnetic moment correction ΔE_{anom}, Eq. (73). Therefore, for the two-photon exchange and screened vacuum-polarization corrections, the off-diagonal matrix element in the *LS* coupling is zero. In this case, the following identity is valid in the jj-coupling scheme [to the order $\alpha^2(\alpha Z)^3$]

$$\sqrt{2}[\Delta E_{(1s2p_{1/2})_1} - \Delta E_{(1s2p_{3/2})_1}] = -\Delta E_{\text{off diag}}^{jj}, \tag{75}$$

where ΔE_i stand for the corresponding matrix elements. For the screened self-energy correction, the off-diagonal matrix element in the *LS* coupling ($\Delta E_{\text{off diag}}^{LS}$) is nonzero and the corresponding identity reads

$$\sqrt{2}[\Delta E_{(1s2p_{1/2})_1} - \Delta E_{(1s2p_{3/2})_1}] + \Delta E_{\text{off diag}}^{jj} = 3\Delta E_{\text{off diag}}^{LS}. \tag{76}$$

Fulfillment of these identities for individual two-electron QED contributions is checked in Table V. For the screened

TABLE IV. Two-electron QED correction for $n=1$ and 2 states of He-like ions, in eV.

Z	State	Scr.SE	Scr.VP	2-ph.exch.	Total	Z	State	Scr.SE	Scr.VP	2-ph.exch.	Total
12	$(1s)^2$	−0.0405	0.0021	0.0031(1)	−0.0353(1)	60	$(1s)^2$	−2.4392(2)	0.3800(1)	0.0662(1)	−1.9930(2)
	$(1s2s)_0$	−0.0088	0.0004	0.0004(1)	−0.0080(1)		$(1s2s)_0$	−0.6267(2)	0.0923	−0.1914(1)	−0.7258(2)
	$(1s2s)_1$	−0.0055	0.0003	−0.0001(1)	−0.0053(1)		$(1s2s)_1$	−0.3377(2)	0.0484	−0.0327(1)	−0.3219(2)
	$(1s2p_{1/2})_0$	−0.0017	0.0001	−0.0008(1)	−0.0024(1)		$(1s2p_{1/2})_0$	−0.1569(1)	0.0311	−0.4945(1)	−0.6203(1)
	$(1s2p_{1/2})_1$	−0.0013	0.0001	−0.0002(1)	−0.0014(1)		$(1s2p_{1/2})_1$	−0.1227(1)	0.0190	−0.1330(1)	−0.2367(1)
	$(1s2p_{3/2})_1$	−0.0010	0.0000	0.0000(1)	−0.0010(1)		$(1s2p_{3/2})_1$	−0.1063(2)	0.0046	−0.0349(1)	−0.1366(2)
	$(1s2p_{3/2})_2$	−0.0025	0.0001	−0.0001(1)	−0.0024(1)		$(1s2p_{3/2})_2$	−0.1666(2)	0.0159	0.0081(1)	−0.1426(2)
	off-diag.	0.0010	−0.0001	0.0001(1)	0.0010(1)		off-diag.	0.0477	−0.0092	0.0053(2)	0.0437(2)
14	$(1s)^2$	−0.0596	0.0034	0.0046(1)	−0.0516(1)	70	$(1s)^2$	−3.8548(1)	0.7130(2)	−0.0164(1)	−3.1581(2)
	$(1s2s)_0$	−0.0131	0.0007	0.0005(1)	−0.0119(1)		$(1s2s)_0$	−1.0358(1)	0.1819	−0.4071(1)	−1.2610(2)
	$(1s2s)_1$	−0.0082	0.0005	−0.0002(1)	−0.0079(1)		$(1s2s)_1$	−0.5321(1)	0.0892	−0.0615(1)	−0.5043(2)
	$(1s2p_{1/2})_0$	−0.0025	0.0002	−0.0015(1)	−0.0037(1)		$(1s2p_{1/2})_0$	−0.3044(1)	0.0667	−0.9717(1)	−1.2094(2)
	$(1s2p_{1/2})_1$	−0.0019	0.0001	−0.0004(1)	−0.0021(1)		$(1s2p_{1/2})_1$	−0.2303(1)	0.0409	−0.2656(1)	−0.4550(2)
	$(1s2p_{3/2})_1$	−0.0016	0.0001	0.0000(1)	−0.0015(1)		$(1s2p_{3/2})_1$	−0.1776(2)	0.0075	−0.0688(1)	−0.2388(2)
	$(1s2p_{3/2})_2$	−0.0037	0.0002	−0.0001(1)	−0.0036(1)		$(1s2p_{3/2})_2$	−0.2588(2)	0.0266	0.0164(1)	−0.2158(2)
	off-diag.	0.0014	−0.0001	0.0002(1)	0.0015(1)		off-diag.	0.0698	−0.0158	0.0063(2)	0.0603(2)
16	$(1s)^2$	−0.0832	0.0051	0.0066(1)	−0.0715(1)	80	$(1s)^2$	−5.9289(1)	1.2980(2)	−0.2374(1)	−4.8682(3)
	$(1s2s)_0$	−0.0184	0.0011	0.0005(1)	−0.0168(1)		$(1s2s)_0$	−1.6738(1)	0.3520(1)	−0.7946(1)	−2.1164(2)
	$(1s2s)_1$	−0.0115	0.0007	−0.0003(1)	−0.0110(1)		$(1s2s)_1$	−0.8173(1)	0.1615(1)	−0.1093(1)	−0.7652(2)
	$(1s2p_{1/2})_0$	−0.0034	0.0003	−0.0025(1)	−0.0056(1)		$(1s2p_{1/2})_0$	−0.5836(1)	0.1429	−1.7938(1)	−2.2345(1)
	$(1s2p_{1/2})_1$	−0.0026	0.0002	−0.0006(1)	−0.0030(1)		$(1s2p_{1/2})_1$	−0.4258(1)	0.0879	−0.4988(1)	−0.8367(1)
	$(1s2p_{3/2})_1$	−0.0022	0.0001	0.0000(1)	−0.0022(1)		$(1s2p_{3/2})_1$	−0.2814(3)	0.0120	−0.1232(1)	−0.3926(3)
	$(1s2p_{3/2})_2$	−0.0052	0.0003	−0.0002(1)	−0.0051(1)		$(1s2p_{3/2})_2$	−0.3839(3)	0.0428	0.0279(1)	−0.3132(3)
	off-diag.	0.0020	−0.0002	0.0003(1)	0.0021(1)		off-diag.	0.0977	−0.0260	0.0072(2)	0.0789(2)
18	$(1s)^2$	−0.1116	0.0072	0.0091(1)	−0.0953(1)	83	$(1s)^2$	−6.7256(1)	1.5500(7)	−0.3460(1)	−5.5216(7)
	$(1s2s)_0$	−0.0248	0.0015	0.0004(1)	−0.0228(1)		$(1s2s)_0$	−1.9289(1)	0.4286(2)	−0.9599(1)	−2.4602(2)
	$(1s2s)_1$	−0.0154	0.0010	−0.0004(1)	−0.0148(1)		$(1s2s)_1$	−0.9273(1)	0.1927(2)	−0.1289(1)	−0.8635(2)
	$(1s2p_{1/2})_0$	−0.0045	0.0004	−0.0039(1)	−0.0080(1)		$(1s2p_{1/2})_0$	−0.7091(1)	0.1799(1)	−2.1377(1)	−2.6669(1)
	$(1s2p_{1/2})_1$	−0.0035	0.0003	−0.0010(1)	−0.0042(1)		$(1s2p_{1/2})_1$	−0.5117(1)	0.1109(1)	−0.5977(1)	−0.9985(1)
	$(1s2p_{3/2})_1$	−0.0031	0.0001	−0.0001(1)	−0.0031(1)		$(1s2p_{3/2})_1$	−0.3201(4)	0.0136	−0.1446(1)	−0.4511(4)
	$(1s2p_{3/2})_2$	−0.0070	0.0004	−0.0002(1)	−0.0068(1)		$(1s2p_{3/2})_2$	−0.4289(4)	0.0489	0.0318(1)	−0.3482(4)
	off-diag.	0.0026	−0.0002	0.0004(1)	0.0028(1)		off-diag.	0.1073	−0.0299	0.0074(4)	0.0848(4)
20	$(1s)^2$	−0.1450	0.0099	0.0119(1)	−0.1231(1)	90	$(1s)^2$	−9.0006(1)	2.338(1)	−0.7109(1)	−7.373(1)
	$(1s2s)_0$	−0.0324	0.0021	0.0003(1)	−0.0300(1)		$(1s2s)_0$	−2.6829(1)	0.6810(2)	−1.4689(1)	−3.4708(3)
	$(1s2s)_1$	−0.0200	0.0014	−0.0006(1)	−0.0192(1)		$(1s2s)_1$	−1.2428(1)	0.2921(2)	−0.1869(1)	−1.1376(2)
	$(1s2p_{1/2})_0$	−0.0059	0.0006	−0.0059(1)	−0.0111(1)		$(1s2p_{1/2})_0$	−1.1197	0.3112(2)	−3.1842(1)	−3.9928(2)
	$(1s2p_{1/2})_1$	−0.0046	0.0004	−0.0015(1)	−0.0057(1)		$(1s2p_{1/2})_1$	−0.7879	0.1929(1)	−0.9024(1)	−1.4974(1)
	$(1s2p_{3/2})_1$	−0.0041	0.0001	−0.0002(1)	−0.0042(1)		$(1s2p_{3/2})_1$	−0.4263(5)	0.0176	−0.2051(1)	−0.6138(5)
	$(1s2p_{3/2})_2$	−0.0092	0.0006	−0.0003(1)	−0.0089(1)		$(1s2p_{3/2})_2$	−0.5496(5)	0.0663	0.0413(1)	−0.4420(5)
	off-diag.	0.0034	−0.0003	0.0005(1)	0.0036(1)		off-diag.	0.1318	−0.0410	0.0082(4)	0.0991(4)
30	$(1s)^2$	−0.3965	0.0348	0.0325(1)	−0.3292(1)	92	$(1s)^2$	−9.7800(1)	2.630(2)	−0.8520(1)	−8.002(2)
	$(1s2s)_0$	−0.0912	0.0076	−0.0048(1)	−0.0884(1)		$(1s2s)_0$	−2.9489(1)	0.7770(4)	−1.6540(1)	−3.8259(4)
	$(1s2s)_1$	−0.0551	0.0048	−0.0024(1)	−0.0527(1)		$(1s2s)_1$	−1.3514(1)	0.3287(2)	−0.2074(1)	−1.2301(3)
	$(1s2p_{1/2})_0$	−0.0166	0.0022	−0.0289(1)	−0.0433(1)		$(1s2p_{1/2})_0$	−1.2775	0.3647(2)	−3.5612(1)	−4.4740(3)
	$(1s2p_{1/2})_1$	−0.0134	0.0013	−0.0074(1)	−0.0195(1)		$(1s2p_{1/2})_1$	−0.8927	0.2262(2)	−1.0133(1)	−1.6798(2)
	$(1s2p_{3/2})_1$	−0.0129	0.0005	−0.0016(1)	−0.0140(1)		$(1s2p_{3/2})_1$	−0.4611(5)	0.0188	−0.2254(1)	−0.6677(5)
	$(1s2p_{3/2})_2$	−0.0261	0.0019	−0.0003(1)	−0.0245(1)		$(1s2p_{3/2})_2$	−0.5886(5)	0.0721	0.0440(1)	−0.4725(5)
	off-diag.	0.0090	−0.0010	0.0013(1)	0.0093(1)		off-diag.	0.1395	−0.0448	0.0084(4)	0.1031(4)

TABLE IV. (*Continued.*)

Z	State	Scr.SE	Scr.VP	2-ph.exch.	Total	Z	State	Scr.SE	Scr.VP	2-ph.exch.	Total
40	$(1s)^2$	−0.8197	0.0887	0.0589(1)	−0.6721(1)	100	$(1s)^2$	−13.6716(1)	4.248(4)	−1.6551(1)	−11.079(4)
	$(1s2s)_0$	−0.1948	0.0199	−0.0252(1)	−0.2002(1)		$(1s2s)_0$	−4.3266(1)	1.3404(8)	−2.6409(1)	−5.6271(8)
	$(1s2s)_1$	−0.1141	0.0118	−0.0068(1)	−0.1091(1)		$(1s2s)_1$	−1.8972(1)	0.5366(5)	−0.3124(1)	−1.6730(5)
	$(1s2p_{1/2})_0$	−0.0378	0.0060	−0.0916(1)	−0.1234(1)		$(1s2p_{1/2})_0$	−2.1876(3)	0.7067(5)	−5.5484(1)	−7.0293(6)
	$(1s2p_{1/2})_1$	−0.0307	0.0036	−0.0239(1)	−0.0510(1)		$(1s2p_{1/2})_1$	−1.4881(3)	0.4408(5)	−1.6074(1)	−2.6547(6)
	$(1s2p_{3/2})_1$	−0.0299	0.0012	−0.0058(1)	−0.0345(1)		$(1s2p_{3/2})_1$	−0.6219(7)	0.0234	−0.3211(1)	−0.9195(7)
	$(1s2p_{3/2})_2$	−0.0553	0.0044	0.0005(1)	−0.0503(1)		$(1s2p_{3/2})_2$	−0.7666(7)	0.1009(1)	0.0529(1)	−0.6128(7)
	off-diag.	0.0179	−0.0025	0.0025(1)	0.0179(1)		off-diag.	0.1728	−0.0630	0.0104(4)	0.1202(4)
50	$(1s)^2$	−1.4717(1)	0.1920	0.0781(1)	−1.2016(1)						
	$(1s2s)_0$	−0.3630(1)	0.0446	−0.0783(1)	−0.3966(1)						
	$(1s2s)_1$	−0.2044(1)	0.0250	−0.0159(1)	−0.1953(1)						
	$(1s2p_{1/2})_0$	−0.0788(1)	0.0141	−0.2289(1)	−0.2936(1)						
	$(1s2p_{1/2})_1$	−0.0632(1)	0.0086	−0.0606(1)	−0.1152(1)						
	$(1s2p_{3/2})_1$	−0.0593(1)	0.0025	−0.0156(1)	−0.0725(1)						
	$(1s2p_{3/2})_2$	−0.1006(1)	0.0088	0.0031(1)	−0.0887(1)						
	off-diag.	0.0306	−0.0050	0.0039(1)	0.0294(1)						

self-energy and vacuum-polarization correction, the fulfillment is obvious from the table. For the two-photon exchange correction, the difference between the right- and left-hand sides is very close to $3(\alpha Z)^4$eV in all cases listed and, therefore, should be ascribed to higher-order contributions, for which the identity is not valid anymore.

III. ENERGIES OF $n=1$ AND $n=2$ STATES OF He-LIKE IONS

In this section we collect all contributions available to the ionization energies of $n=1$ and 2 states of He-like ions. Individual corrections for selected ions are listed in Table VI. A description of contributions presented there is given below.

Dirac energy. $\Delta E_{\rm Dirac}$ is the Dirac value for the ionization energy of the valence electron including the finite-nuclear-size effect. The energy levels were calculated employing the two-parameter Fermi model for the nuclear-charge distribution. Parameters of the Fermi model were expressed in terms of the root-mean-square (rms) radius (see, e.g., Ref. [57]). The actual values of rms radii as well as their uncertainties were taken from a recent tabulation [58]. In a few cases of Z with no experimental data available we employed values for the rms radii obtained by the approximate formula from Ref. [59] and ascribed an uncertainty of 1% to them. For each value of Z, the nuclear parameters for the isotope with the largest abundance (with the longest lifetime) were chosen. The uncertainty of the nuclear-size effect was evaluated by adding quadratically two errors, one obtained by varying the rms radius within its error bars and the other obtained by changing the model of the nuclear-charge distribution (the Fermi and the homogeneously-charged-sphere model were employed). Numerical values of fundamental constants used in the calculation were [60] $\alpha^{-1}=137.035\,999\,11(46)$ and $hcR_\infty=13.605\,692\,3(12)$eV.

Electron-electron interaction correction. $\Delta E_{\rm int}$ incorporates corrections that can be derived from the Breit equation. It consists of three parts,

$$\Delta E_{\rm int}=\Delta E_{\rm 1ph}+\Delta E_{\rm 2ph}^{\rm Breit}+\Delta E_{\geqslant 3{\rm ph}}^{\rm Breit}, \tag{77}$$

which correspond to the one-, two-, and three- and more photon exchange, respectively. In the notations of Sec. I, the one-photon exchange correction is written as [35,47]

$$\Delta E_{\rm 1ph}=\frac{1}{2}\sum_P (-1)^P[I_{Pi_1Pi_2k_1k_2}(\Delta_1)+I_{Pi_1Pi_2k_1k_2}(\Delta_2)], \tag{78}$$

where $\Delta_1=\varepsilon_{Pi_1}-\varepsilon_{k_1}$ and $\Delta_2=\varepsilon_{Pi_2}-\varepsilon_{k_2}$. Its numerical evaluation was carried out employing the Fermi model for the nuclear-charge distribution; accurate numerical results for this correction can be found in Ref. [39]. In this paper we recalculated this correction using new values of the nuclear radii [58]. Its uncertainty was estimated in the same way as in the case of the Dirac energy. $\Delta E_{\rm 2ph}^{\rm Breit}$ represents the two-photon exchange correction within the $\alpha^2(\alpha Z)^2$ approximation and is given by the first two terms in Eq. (71), with the coefficients a_0 and a_2 listed in Table III. The contribution due to the exchange by three and more photons was evaluated by summing terms of the $1/Z$ expansion, with the corresponding coefficients taken from Refs. [53,54] for the nonrelativistic energy and from Ref. [18] for the Breit-Pauli correction.

One-electron QED correction. $\Delta E_{\rm 1el}^{\rm QED}$ is the sum of the one-loop and two-loop one-electron QED corrections. The one-loop self-energy correction for $1s, 2s$, and $2p_{1/2}$ states and $Z\geqslant 26$ (including the nuclear-size effect) was tabulated in Ref. [61] by using the method developed by Mohr and co-workers [14,62,63]. For lower values of Z and for the $2p_{3/2}$ state, we used a combination of our own calculation and an interpolation of the point-nucleus results from Ref.

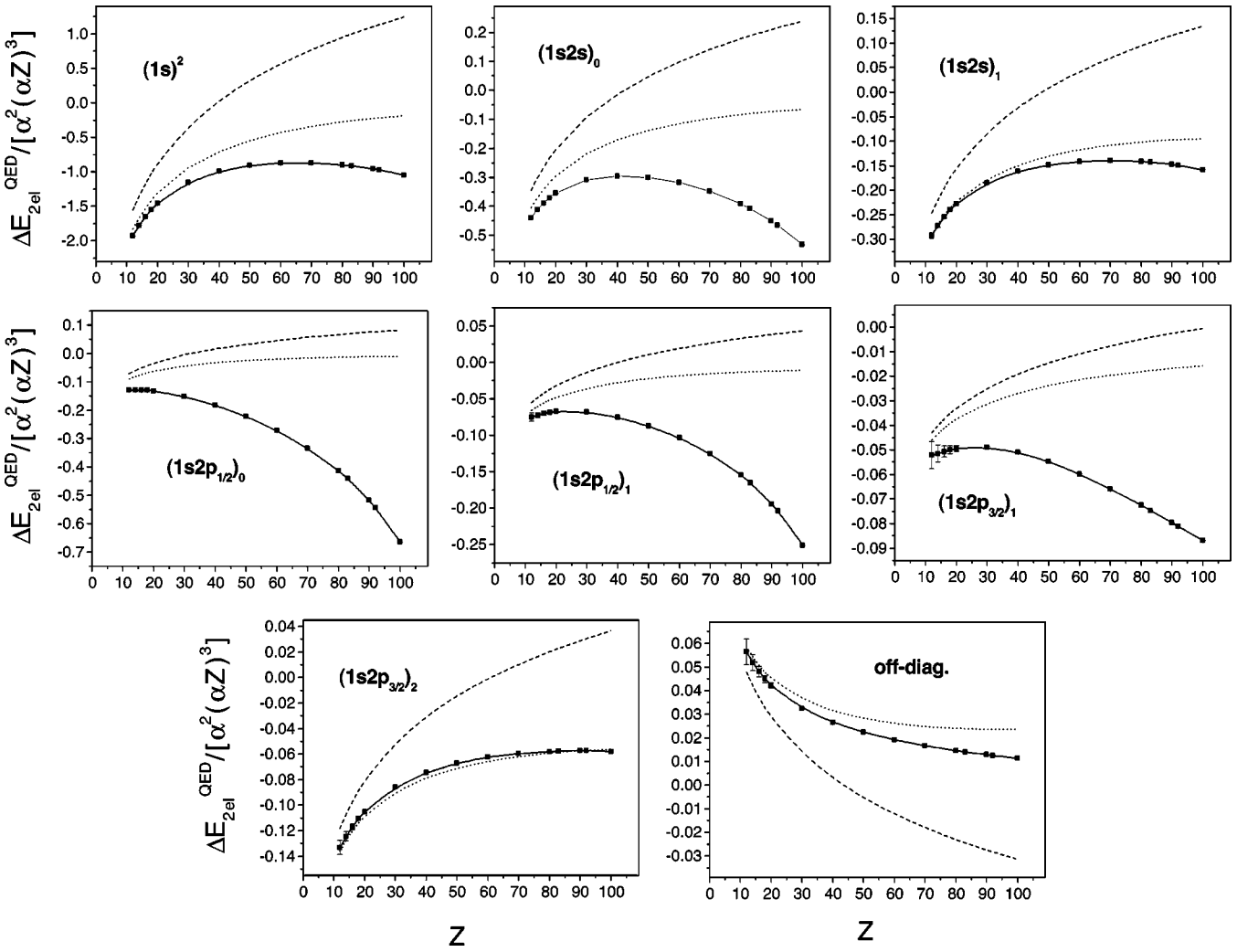

FIG. 4. Comparison of our all-order numerical results for the second-order two-electron QED correction (square dots, solid line) with values for this correction within the αZ expansion [the contribution of order $\alpha^2(\alpha Z)^3$, dashed line] and with the related QED contribution by Drake [18] (dotted line), in units of $\alpha^2(\alpha Z)^3$.

[64]. The Uehling part of the one-loop vacuum-polarization correction was calculated in this work for the Fermi nuclear model. The Wichmann-Kroll part of the vacuum-polarization correction was tabulated for $Z \geqslant 30$ in Ref. [65]. For lower values of Z, it was calculated in this work by employing the

TABLE V. Right-hand side (RHS) and left-hand side (LHS) of Eq. (76) (for the screened self-energy correction) and those of Eq. (75) (for the screened vacuum-polarization and two-photon exchange corrections), in eV. The comparison is valid to the leading order in αZ only. The last column demonstrates that the difference (RHS−LHS) for the two-photon exchange correction arises predominantly from effects to order $\alpha^2(\alpha Z)^4$.

Z	Scr.SE		Scr.VP		2-ph.exch.		
	LHS	RHS	LHS	RHS	LHS	RHS	$(\mathrm{RHS}-\mathrm{LHS})/(\alpha Z)^4$
12	0.0006	0.0006	0.0001	0.0001	−0.0003	−0.0001	3
14	0.0010	0.0009	0.0001	0.0001	−0.0005	−0.0002	3
16	0.0014	0.0013	0.0002	0.0002	−0.0008	−0.0003	3.0
18	0.0020	0.0019	0.0002	0.0002	−0.0012	−0.0004	3.0
20	0.0027	0.0026	0.0003	0.0003	−0.0018	−0.0005	3.0
30	0.0083	0.0087	0.0012	0.0010	−0.0083	−0.0013	3.0
40	0.0167	0.0205	0.0035	0.0025	−0.0256	−0.0025	3.18

TABLE VI. Individual contributions to the ionization energies of He-like ions (with the opposite sign), in eV. For mixing configurations, contributions to the matrix elements are listed.

Z	State	$\Delta E_{\mathrm{Dirac}}$	ΔE_{int}	$\Delta E_{\mathrm{1el}}^{\mathrm{QED}}$	$\Delta E_{\mathrm{2el}}^{\mathrm{QED}}$	$\Delta E_{\mathrm{ho}}^{\mathrm{QED}}$	ΔE_{rec}	Total
12	$(1s)^2$	−1962.9888(1)	200.8973	0.2801	−0.0353(1)	0.0008	0.0412	−1761.8047(2)
	$(1s2s)_0$	−490.9832	72.9751	0.0371	−0.0080(1)	0.0005	0.0096	−417.9689(1)
	$(1s2s)_1$	−490.9832	60.2485	0.0371	−0.0053(1)	0.0001	0.0099	−430.6929(1)
	$(1s2p_{1/2})_0$	−490.9834	72.1736	−0.0010	−0.0024(1)	0.0002	0.0037	−418.8092(1)
	$(1s2p_{1/2})_1$	−490.9834	74.9742	−0.0010	−0.0014(1)	0.0002	0.0075	−416.0038(1)
	$(1s2p_{3/2})_1$	−490.0399	77.7699	0.0012	−0.0010(1)	0.0001	0.0113	−412.2584(1)
	$(1s2p_{3/2})_2$	−490.0399	71.7742	0.0012	−0.0024(1)	0.0003	0.0036	−418.2630(1)
	off-diag.	0	4.1676	0	0.0010(1)	−0.0001	0.0054	4.1739(1)
14	$(1s)^2$	−2673.7079(2)	235.5743	0.4778	−0.0516(1)	0.0008	0.0487	−2437.6579(2)
	$(1s2s)_0$	−668.8651	85.8199	0.0637	−0.0119(1)	0.0006	0.0115	−582.9812(1)
	$(1s2s)_1$	−668.8651	70.5889	0.0637	−0.0079(1)	0.0002	0.0118	−598.2084(1)
	$(1s2p_{1/2})_0$	−668.8654	84.7684	−0.0017	−0.0037(1)	0.0002(1)	0.0044	−584.0978(1)
	$(1s2p_{1/2})_1$	−668.8654	88.0659	−0.0017	−0.0021(1)	0.0002	0.0090	−580.7942(1)
	$(1s2p_{3/2})_1$	−667.1144	91.3603	0.0022	−0.0015(1)	0.0001	0.0135	−575.7398(1)
	$(1s2p_{3/2})_2$	−667.1144	84.1211	0.0022	−0.0036(1)	0.0004	0.0043	−582.9900(1)
	off-diag.	0	5.0013	0	0.0015(1)	−0.0002	0.0065	5.0091(1)
16	$(1s)^2$	−3495.0044(3)	270.4822	0.7562	−0.0715(1)	0.0009	0.0563	−3223.7804(3)
	$(1s2s)_0$	−874.5000	98.7466	0.1014	−0.0168(1)	0.0007	0.0134	−775.6548(1)
	$(1s2s)_1$	−874.5000	80.9665	0.1014	−0.0110(1)	0.0002	0.0137	−793.4292(1)
	$(1s2p_{1/2})_0$	−874.5006	97.4677	−0.0028	−0.0056(1)	0.0003(2)	0.0051	−777.0360(2)
	$(1s2p_{1/2})_1$	−874.5006	101.2216	−0.0028	−0.0030(1)	0.0003	0.0105	−773.2742(1)
	$(1s2p_{3/2})_1$	−871.5075	104.9765	0.0038	−0.0022(1)	0.0001	0.0158	−766.5134(1)
	$(1s2p_{3/2})_2$	−871.5075	96.4856	0.0038	−0.0051(1)	0.0005	0.0051	−775.0176(1)
	off-diag.	0	5.8246	0	0.0021(1)	−0.0002	0.0076	5.8341(1)
18	$(1s)^2$	−4427.4154(3)	305.6560	1.1310(1)	−0.0953(1)	0.0009	0.0575	−4120.6653(4)
	$(1s2s)_0$	−1108.0563	111.7675	0.1525	−0.0228(1)	0.0007(1)	0.0138	−996.1446(2)
	$(1s2s)_1$	−1108.0563	91.3873	0.1525	−0.0148(1)	0.0003	0.0141	−1016.5170(1)
	$(1s2p_{1/2})_0$	−1108.0575	110.2884	−0.0043	−0.0080(1)	0.0003(3)	0.0053	−997.7758(3)
	$(1s2p_{1/2})_1$	−1108.0575	114.4514	−0.0043	−0.0042(1)	0.0003	0.0108	−993.6035(1)
	$(1s2p_{3/2})_1$	−1103.2520	118.6220	0.0062	−0.0031(1)	0.0001	0.0162	−984.6106(1)
	$(1s2p_{3/2})_2$	−1103.2520	108.8712	0.0062	−0.0068(1)	0.0005	0.0052	−994.3757(1)
	off-diag.	0	6.6353	0	0.0028(1)	−0.0002	0.0078	6.6456(1)
20	$(1s)^2$	−5471.5561(4)	341.1315	1.6179(2)	−0.1231(1)	0.0008	0.0715	−5128.8573(5)
	$(1s2s)_0$	−1369.7266(1)	124.8955	0.2195(1)	−0.0300(1)	0.0008(1)	0.0172	−1244.6236(2)
	$(1s2s)_1$	−1369.7266(1)	101.8571	0.2195(1)	−0.0192(1)	0.0003	0.0175	−1267.6514(2)
	$(1s2p_{1/2})_0$	−1369.7284(1)	123.2478	−0.0063	−0.0111(1)	0.0004(4)	0.0066	−1246.4911(4)
	$(1s2p_{1/2})_1$	−1369.7284(1)	127.7657	−0.0063	−0.0057(1)	0.0003(1)	0.0135	−1241.9609(2)
	$(1s2p_{3/2})_1$	−1362.3854(1)	132.3004	0.0097	−0.0042(1)	0.0001	0.0203	−1230.0591(1)
	$(1s2p_{3/2})_2$	−1362.3854(1)	121.2809	0.0097	−0.0089(1)	0.0006	0.0065	−1241.0966(1)
	off-diag.	0	7.4312	0	0.0036(1)	−0.0003	0.0097	7.4442(1)
30	$(1s)^2$	−12395.3524(11)	524.3343	6.3051(15)	−0.3292(1)	−0.0002	0.1036	−11864.9387(19)
	$(1s2s)_0$	−3108.3051(2)	192.6165	0.8826(14)	−0.0884(1)	0.0010(4)	0.0254	−2914.8681(15)
	$(1s2s)_1$	−3108.3051(2)	155.1569	0.8826(14)	−0.0527(1)	0.0005	0.0257	−2952.2921(14)
	$(1s2p_{1/2})_0$	−3108.3194(2)	190.7532	−0.0229(3)	−0.0433(1)	0.0006(15)	0.0099	−2917.6219(15)
	$(1s2p_{1/2})_1$	−3108.3194(2)	195.9800	−0.0229(3)	−0.0195(1)	0.0006(5)	0.0199	−2912.3614(7)
	$(1s2p_{3/2})_1$	−3070.5058(2)	201.3173	0.0546(3)	−0.0140(1)	0.0001	0.0295	−2869.1183(4)
	$(1s2p_{3/2})_2$	−3070.5058(2)	183.7940	0.0546(3)	−0.0245(1)	0.0012	0.0096	−2886.6710(4)
	off-diag.	0	11.1222	0	0.0093(1)	−0.0006	0.0140	11.1450(1)

TABLE VI. (*Continued.*)

Z	State	$\Delta E_{\mathrm{Dirac}}$	ΔE_{int}	$\Delta E_{1\mathrm{el}}^{\mathrm{QED}}$	$\Delta E_{2\mathrm{el}}^{\mathrm{QED}}$	$\Delta E_{\mathrm{ho}}^{\mathrm{QED}}$	ΔE_{rec}	Total
40	$(1s)^2$	−22253.1584(20)	720.9167	16.3146(49)	−0.6721(1)	−0.0030(12)	0.1354	−21516.4668(55)
	$(1s2s)_0$	−5593.9687(4)	265.1795	2.3647(68)	−0.2002(1)	0.0007(5)	0.0334	−5326.5905(68)
	$(1s2s)_1$	−5593.9687(4)	210.6535	2.3647(68)	−0.1091(1)	0.0008	0.0338	−5381.0250(68)
	$(1s2p_{1/2})_0$	−5594.0371(4)	264.5842	−0.0397(16)	−0.1234(1)	0.0008(37)	0.0134	−5329.6018(40)
	$(1s2p_{1/2})_1$	−5594.0371(4)	268.0222	−0.0397(16)	−0.0510(1)	0.0007(12)	0.0260	−5326.0789(21)
	$(1s2p_{3/2})_1$	−5471.5706(4)	271.7375	0.1925(16)	−0.0345(1)	0.0001	0.0378	−5199.6372(16)
	$(1s2p_{3/2})_2$	−5471.5706(4)	247.3426	0.1925(16)	−0.0503(1)	0.0018	0.0125	−5224.0715(16)
	off-diag.	0	14.1717	0	0.0179(1)	−0.0010(1)	0.0178	14.2065(1)
50	$(1s)^2$	−35226.6126(39)	936.5561	33.9605(80)	−1.2016(1)	−0.0077(50)	0.1659	−34257.139(10)
	$(1s2s)_0$	−8884.1001(8)	344.7874	5.118(22)	−0.3966(1)	−0.0001	0.0412	−8534.551(22)
	$(1s2s)_1$	−8884.1001(8)	269.3107	5.118(22)	−0.1953(1)	0.0011(1)	0.0415	−8609.825(22)
	$(1s2p_{1/2})_0$	−8884.3682(7)	347.6604	−0.0064(49)	−0.2936(1)	0.0009(77)	0.0170	−8536.9898(91)
	$(1s2p_{1/2})_1$	−8884.3682(7)	345.6502	−0.0064(49)	−0.1152(1)	0.0009(26)	0.0315	−8538.8072(56)
	$(1s2p_{3/2})_1$	−8575.5142(7)	344.0792	0.5228(49)	−0.0725(1)	−0.0002(2)	0.0447	−8230.9403(49)
	$(1s2p_{3/2})_2$	−8575.5142(7)	312.2765	0.5228(49)	−0.0887(1)	0.0025(1)	0.0152	−8262.7860(49)
	off-diag.	0	16.3734	0	0.0294(1)	−0.0015(3)	0.0206	16.4220(3)
60	$(1s)^2$	−51577.900(12)	1178.1906(3)	61.917(21)	−1.9930(2)	−0.014(15)	0.2152	−50339.584(28)
	$(1s2s)_0$	−13062.0774(19)	434.2619	9.742(52)	−0.7258(2)	−0.0014(24)	0.0537	−12618.747(52)
	$(1s2s)_1$	−13062.0774(19)	332.3353	9.742(52)	−0.3219(2)	0.0015(3)	0.0541	−12720.266(52)
	$(1s2p_{1/2})_0$	−13062.9669(11)	443.7640	0.202(12)	−0.6203(1)	0.001(14)	0.0227	−12619.597(19)
	$(1s2p_{1/2})_1$	−13062.9669(11)	431.1433	0.202(12)	−0.2367(1)	0.0010(46)	0.0400	−12631.817(13)
	$(1s2p_{3/2})_1$	−12395.4634(10)	418.8976	1.199(12)	−0.1366(2)	−0.0005(9)	0.0546	−11975.449(12)
	$(1s2p_{3/2})_2$	−12395.4634(10)	378.9464	1.199(12)	−0.1426(2)	0.0034(1)	0.0193	−12015.438(12)
	off-diag.	0	17.5341	0	0.0437(2)	−0.0021(5)	0.0246	17.6002(6)
70	$(1s)^2$	−71678.288(49)	1454.7183(14)	103.454(51)	−3.1581(2)	−0.023(36)	0.2612	−70123.037(79)
	$(1s2s)_0$	−18247.2685(78)	537.4109(3)	17.07(10)	−1.2610(2)	−0.0033(84)	0.0658	−17693.98(10)
	$(1s2s)_1$	−18247.2685(78)	401.3107(2)	17.07(10)	−0.5043(2)	0.0019(5)	0.0662	−17829.32(10)
	$(1s2p_{1/2})_0$	−18250.1829(16)	558.0870(1)	0.844(27)	−1.2094(2)	0.001(25)	0.0283	−17692.432(36)
	$(1s2p_{1/2})_1$	−18250.1829(16)	527.6353	0.844(27)	−0.4550(2)	0.0011(74)	0.0469	−17722.111(28)
	$(1s2p_{3/2})_1$	−16948.0262(15)	496.7903	2.443(27)	−0.2388(2)	−0.0010(24)	0.0608	−16448.972(27)
	$(1s2p_{3/2})_2$	−16948.0262(15)	447.7120	2.443(27)	−0.2158(2)	0.0043(1)	0.0225	−16498.060(27)
	off-diag.	0	17.4749	0	0.0603(2)	−0.0030(9)	0.0266	17.5589(9)
80	$(1s)^2$	−96061.23(11)	1778.3471(31)	162.76(12)	−4.8682(3)	−0.035(78)	0.3326	−94124.69(18)
	$(1s2s)_0$	−24612.835(18)	659.7046(9)	28.31(16)	−2.1164(2)	−0.006(21)	0.0853	−23926.85(16)
	$(1s2s)_1$	−24612.835(18)	478.4429(4)	28.31(16)	−0.7652(2)	0.0023(9)	0.0858	−24106.75(16)
	$(1s2p_{1/2})_0$	−24621.4113(26)	698.2095(2)	2.411(52)	−2.2345(1)	0.001(41)	0.0369	−23922.987(66)
	$(1s2p_{1/2})_1$	−24621.4113(26)	639.7158(1)	2.411(52)	−0.8367(1)	0.001(11)	0.0570	−23980.063(53)
	$(1s2p_{3/2})_1$	−22253.6744(19)	578.4001	4.557(52)	−0.3926(3)	−0.0017(52)	0.0686	−21671.044(52)
	$(1s2p_{3/2})_2$	−22253.6744(19)	518.9618(1)	4.557(52)	−0.3132(3)	0.0054(1)	0.0267	−21730.437(52)
	off-diag.	0	16.0289	0	0.0789(2)	−0.0040(15)	0.0289	16.133(2)
83	$(1s)^2$	−104318.39(16)	1887.0407(45)	184.80(15)	−5.5216(7)	−0.038(96)	0.3620	−102251.76(24)
	$(1s2s)_0$	−26788.017(27)	701.2559(13)	32.69(18)	−2.4602(2)	−0.007(27)	0.0938	−26056.44(18)
	$(1s2s)_1$	−26788.017(27)	503.6149(6)	32.69(18)	−0.8635(2)	0.0025(10)	0.0943	−26252.48(18)
	$(1s2p_{1/2})_0$	−26799.9148(34)	746.8798(4)	3.183(62)	−2.6669(1)	0.001(47)	0.0404	−26052.477(79)
	$(1s2p_{1/2})_1$	−26799.9148(34)	677.3539(2)	3.183(62)	−0.9985(1)	0.001(12)	0.0611	−26120.315(64)
	$(1s2p_{3/2})_1$	−23995.8088(21)	603.7087	5.416(62)	−0.4511(4)	−0.0020(63)	0.0715	−23387.066(63)
	$(1s2p_{3/2})_2$	−23995.8088(21)	540.8844(1)	5.416(62)	−0.3482(4)	0.0057	0.0283	−23449.823(63)
	off-diag.	0	15.3020(1)	0	0.0848(4)	−0.0043(17)	0.0297	15.412(2)

TABLE VI. (*Continued.*)

Z	State	$\Delta E_{\mathrm{Dirac}}$	ΔE_{int}	$\Delta E_{1\mathrm{el}}^{\mathrm{QED}}$	$\Delta E_{2\mathrm{el}}^{\mathrm{QED}}$	$\Delta E_{\mathrm{ho}}^{\mathrm{QED}}$	ΔE_{rec}	Total
90	$(1s)^2$	−125498.8(2.1)	2166.546(61)	245.28(27)	−7.3734(10)	−0.05(16)	0.4338	−123094.1(2.1)
	$(1s2s)_0$	−32414.63(39)	809.386(19)	45.19(21)	−3.4708(3)	−0.009(45)	0.1168	−31563.44(45)
	$(1s2s)_1$	−32414.63(39)	566.9253(84)	45.19(21)	−1.1376(2)	0.0029(14)	0.1174	−31803.55(44)
	$(1s2p_{1/2})_0$	−32440.630(43)	875.9251(68)	5.824(93)	−3.9928(2)	0.002(66)	0.0496	−31562.83(12)
	$(1s2p_{1/2})_1$	−32440.630(43)	774.5637(43)	5.824(93)	−1.4974(1)	0.001(16)	0.0707	−31661.67(10)
	$(1s2p_{3/2})_1$	−28337.2423(25)	664.4054(1)	7.930(93)	−0.6138(5)	−0.0026(97)	0.0759	−27665.450(94)
	$(1s2p_{3/2})_2$	−28337.2423(25)	593.1309(17)	7.930(93)	−0.4420(5)	0.0066	0.0314	−27736.588(93)
	off-diag.	0	13.0484(12)	0	0.0991(4)	−0.0052(23)	0.0305	13.170(3)
92	$(1s)^2$	−132081.59(52)	2253.940(15)	265.16(33)	−8.0020(20)	−0.05(18)	0.4600	−129570.30(64)
	$(1s2s)_0$	−34177.81(10)	843.6097(49)	49.44(22)	−3.8259(4)	−0.009(51)	0.1260	−33288.51(24)
	$(1s2s)_1$	−34177.81(10)	586.3566(21)	49.44(22)	−1.2301(3)	0.0030(16)	0.1266	−33543.15(24)
	$(1s2p_{1/2})_0$	−34211.077(12)	917.4978(17)	6.86(10)	−4.4740(3)	0.002(73)	0.0531	−33291.14(13)
	$(1s2p_{1/2})_1$	−34211.077(12)	805.1940(11)	6.86(10)	−1.6798(2)	0.001(17)	0.0743	−33400.63(11)
	$(1s2p_{3/2})_1$	−29649.8353(26)	682.1945	8.80(10)	−0.6677(5)	−0.003(11)	0.0774	−28959.44(10)
	$(1s2p_{3/2})_2$	−29649.8353(26)	608.3559(4)	8.80(10)	−0.4725(5)	0.0068	0.0324	−29033.12(10)
	off-diag.	0	12.2590(2)	0	0.1031(4)	−0.0054(25)	0.0308	12.383(3)
100	$(1s)^2$	−161165.5(6.1)	2646.56(18)	358.30(63)	−11.0787(40)	−0.06(30)	0.6180	−158171.1(6.1)
	$(1s2s)_0$	−42048.7(1.3)	999.862(63)	70.19(20)	−5.6271(8)	−0.012(86)	0.1895	−40984.1(1.3)
	$(1s2s)_1$	−42048.7(1.3)	671.724(25)	70.19(20)	−1.6730(5)	0.0035(23)	0.1902	−41308.3(1.3)
	$(1s2p_{1/2})_0$	−42127.25(19)	1111.129(25)	12.82(16)	−7.0293(6)	0.00(11)	0.0759	−41010.25(27)
	$(1s2p_{1/2})_1$	−42127.25(19)	944.380(16)	12.82(16)	−2.6547(6)	0.001(21)	0.0984	−41172.61(25)
	$(1s2p_{3/2})_1$	−35228.5701(31)	755.4923(2)	13.05(16)	−0.9195(7)	−0.004(16)	0.0866	−34460.87(16)
	$(1s2p_{3/2})_2$	−35228.5701(31)	670.7582(42)	13.05(16)	−0.6128(7)	0.0079(2)	0.0382	−34545.33(16)
	off-diag.	0	8.4030(29)	0	0.1202(4)	−0.0066(34)	0.0328	8.550(5)

asymptotic-expansion formulas for the Wichmann-Kroll potential [66].

The two-loop one-electron QED correction is calculated to all orders in αZ only for the $1s$ state up to now (see Ref. [51] and references therein). For excited states, one has to rely on the αZ expansion, which reads (see the review [67], references therein, and more recent studies [68–70])

$$\Delta E_{1\mathrm{el},2\mathrm{lo}}^{\mathrm{QED}} = \frac{\alpha^2}{\pi^2}\frac{(\alpha Z)^4}{n^3}\{B_{40} + (\alpha Z)B_{50} + (\alpha Z)^2[L^3 B_{63} + L^2 B_{62} + L\, B_{61} + G_{2\mathrm{lo}}^{\mathrm{ho}}(\alpha Z)]\}, \tag{79}$$

where $L=\ln[(\alpha Z)^{-2}]$, $G_{2\mathrm{lo}}^{\mathrm{ho}}(\alpha Z)=B_{60}+(\alpha Z)(\cdots)$ is the higher-order remainder, and the coefficients B_{ij} are

$$B_{40} = \left[2\pi^2\ln 2 - \frac{49}{108}\pi^2 - \frac{6131}{1296} - 3\zeta(3)\right]\delta_{l0} + \left[\frac{1}{2}\pi^2\ln 2 - \frac{1}{12}\pi^2 - \frac{197}{144} - \frac{3}{4}\zeta(3)\right]\frac{1}{\kappa(2l+1)}, \tag{80}$$

$$B_{50} = -21.5561(31)\,\delta_{l0}, \tag{81}$$

$$B_{63} = -\frac{8}{27}\delta_{l0}, \tag{82}$$

$$B_{62}(ns) = \frac{16}{9}\left(\frac{71}{60} - \ln(2n) + \frac{1}{4n^2} - \frac{1}{n} + \psi(n) + C\right), \tag{83}$$

$$B_{62}(np) = \frac{4}{27}\frac{n^2-1}{n^2}, \tag{84}$$

$$B_{61}(1s) = 50.344\,005, \tag{85}$$

$$B_{61}(2s) = 42.447\,669, \tag{86}$$

$$B_{60}(1s) = -61.6(9), \tag{87}$$

$$B_{60}(2s) = -53.2(8), \tag{88}$$

where ζ is the Riemann zeta function, ψ is the logarithmic derivative of the gamma function, and $C=0.577\,215\,66\ldots$ is the Euler constant. Great care should be taken employing the αZ expansion for the estimation of the total correction for middle- and high-Z ions, due to a very slow convergence of this expansion. In addition, it was found lately [71] that the numerical all-order results do not agree well with the analytical calculations to order $\alpha^2(\alpha Z)^6$. A possible reason for this disagreement [72] can be the incompleteness of the analytical results (85) and (86) for the B_{61} coefficient.

In order to extrapolate the all-order numerical results of Ref. [51] to the region $Z=12$–39 for the $1s$ state and to

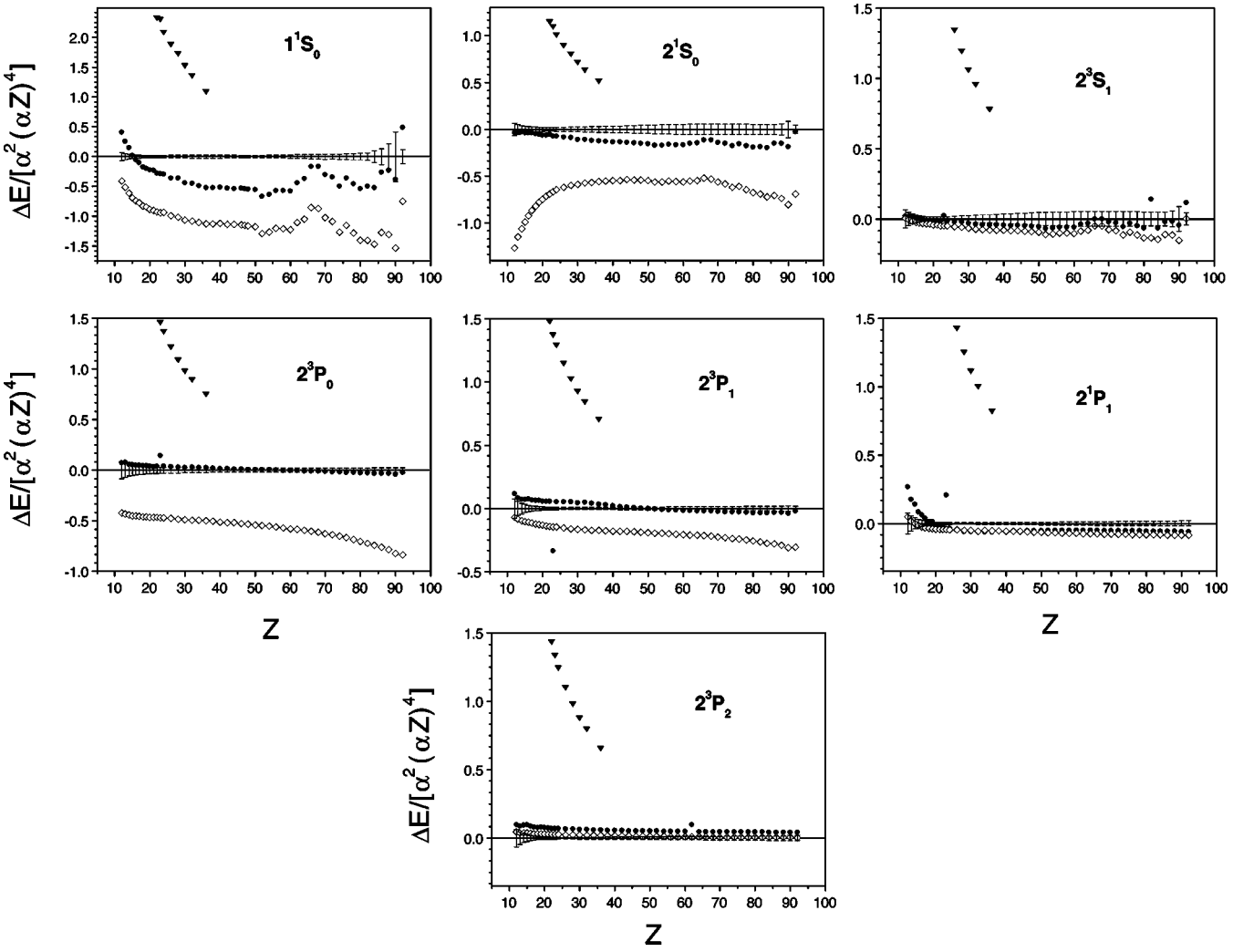

FIG. 5. Comparison of different evaluations for the total ionization energy of $n=1$ and 2 states of He-like ions. Plotted is the difference between the results obtained by us and by other authors, normalized by the factor $\alpha^2(\alpha Z)^4$. Error bars refer to the estimation of the uncertainty of the present evaluation, open diamonds denote the results by Drake [18], filled circles stand for those by Plante *et al.* [21], and filled triangles indicate the values by Cheng and Chen [24].

estimate the two-loop correction for excited states, we separate the 1*s* higher-order remainder $G^{\rm ho}_{\rm 2lo}(\alpha Z)$ from the numerical data of Ref. [51]. We observe that this function is smoothly behaving and can be reasonably approximated by a polynomial. We thus employ a linear (parabolic) fit to the function $G^{\rm ho}_{\rm 2lo}(\alpha Z)$ in order to extrapolate the higher-order contribution to the region $Z=12$–39. For the 2*s* state, we employ the same values for the higher-order contribution and ascribe an uncertainty of 50% to them. For *p* states, no analytical calculations for the B_{61} coefficient exist up to now. We thus separate from the 1*s* numerical results of Ref. [51] the function

$$\tilde{G}^{\rm ho}_{\rm 2lo}(\alpha Z) = L\, B_{61} + G^{\rm ho}_{\rm 2lo}(\alpha Z), \tag{89}$$

divide it by a factor of 8, and take the result as the uncertainty for the higher-order contribution for *p* states.

Two-electron QED correction. $\Delta E^{\rm QED}_{\rm 2el}$ is evaluated in Sec. II; the data are taken from Table IV.

Higher-order QED correction. $\Delta E^{\rm QED}_{\rm ho}$ represents the contribution of QED effects of relative order $1/Z^2$ and higher. This correction was evaluated by formulas presented in Ref. [18] suppressing terms that contribute to orders $1/Z^0$ and $1/Z$. Its uncertainty was obtained by taking the relative deviation of the QED contribution to order $1/Z$ calculated according to Ref. [18] from the results of its exact evaluation presented in this work. (The corresponding comparison is presented in Fig. 4.)

Relativistic recoil correction. $\Delta E_{\rm rec}$ consists of the one-electron and the two-electron part. The one-electron relativistic recoil correction was evaluated to all orders in αZ in a series of papers [73–75]. In our compilation, we employed the finite-nucleus results of Ref. [75] for the 1*s* state, the point-nucleus results of Ref. [73] for the 2*s* and $2p_{1/2}$ states, and those of Ref. [74] for the $2p_{3/2}$ state. The two-electron recoil contribution is given by the sum of the mass-polarization correction and the electron-electron interaction correction to the one-electron nuclear recoil. The nonrelativistic part of the mass-polarization correction was evaluated by summing the terms of the $1/Z$ expansion of the matrix

TABLE VII. Total ionization energies (in eV) for $n=1$ and 2 states of He-like ions. "rms" denotes the root-mean-square radii expressed in fermis.

Z	rms	$1\,^1S_0$	$2\,^1S_0$	$2\,^3S_1$	$2\,^3P_0$	$2\,^3P_1$	$2\,^1P_1$	$2\,^3P_2$
12	3.057	1761.8047(2)	417.9689(1)	430.6929(1)	418.8092(1)	418.7059(1)	409.5564(1)	418.2630(1)
13	3.061	2085.9768(2)	497.0265(1)	510.9969(1)	498.0060(1)	497.8514(1)	487.6854(1)	497.2157(1)
14	3.122	2437.6579(2)	582.9812(1)	598.2084(1)	584.0978(1)	583.8775(1)	572.6565(1)	582.9900(1)
15	3.189	2816.9085(2)	675.8517(1)	692.3466(1)	677.1019(2)	676.8003(1)	664.4775(1)	675.5897(1)
16	3.261	3223.7804(3)	775.6548(1)	793.4292(1)	777.0360(2)	776.6365(1)	763.1512(1)	775.0176(1)
17	3.365	3658.3434(3)	882.4120(1)	901.4786(1)	883.9202(2)	883.4062(1)	868.6849(1)	881.2783(1)
18	3.427	4120.6653(4)	996.1446(2)	1016.5170(1)	997.7758(3)	997.1309(1)	981.0832(1)	994.3757(1)
19	3.435	4610.8069(4)	1116.8727(2)	1138.5652(1)	1118.6243(3)	1117.8333(1)	1100.3453(1)	1114.3132(1)
20	3.476	5128.8573(5)	1244.6236(2)	1267.6514(2)	1246.4911(4)	1245.5404(1)	1226.4796(1)	1241.0966(1)
21	3.544	5674.9031(6)	1379.4241(3)	1403.8034(2)	1381.4022(5)	1380.2811(2)	1359.4907(1)	1374.7311(1)
22	3.591	6249.0219(6)	1521.2994(3)	1547.0473(3)	1523.3841(6)	1522.0846(2)	1499.3778(1)	1515.2211(1)
23	3.599	6851.3102(7)	1670.2795(4)	1697.4140(3)	1672.4661(6)	1670.9838(2)	1646.1449(2)	1662.5724(2)
24	3.642	7481.8620(8)	1826.3945(5)	1854.9344(4)	1828.6785(7)	1827.0129(3)	1799.7936(2)	1816.7905(2)
25	3.706	8140.7864(10)	1989.6781(6)	2019.6432(5)	1992.0540(8)	1990.2087(3)	1960.3291(2)	1977.8821(2)
26	3.737	8828.1870(11)	2160.1631(7)	2191.5744(6)	2162.6260(10)	2160.6084(4)	2127.7523(2)	2145.8531(2)
27	3.788	9544.1823(13)	2337.8867(8)	2370.7659(8)	2340.4308(11)	2338.2524(4)	2302.0690(3)	2320.7105(3)
28	3.775	10288.8852(14)	2522.8845(10)	2557.2545(10)	2525.5048(12)	2523.1804(5)	2483.2799(3)	2502.4606(3)
29	3.882	11062.4302(16)	2715.1990(12)	2751.0835(12)	2717.8887(14)	2715.4373(5)	2671.3953(4)	2691.1121(4)
30	3.929	11864.9387(19)	2914.8681(15)	2952.2921(14)	2917.6219(15)	2915.0647(6)	2866.4149(4)	2886.6710(4)
31	3.997	12696.5562(21)	3121.9374(17)	3160.9270(17)	3124.7482(17)	3122.1101(7)	3068.3490(5)	3089.1463(5)
32	4.074	13557.4194(24)	3336.4505(21)	3377.0326(20)	3339.3120(19)	3336.6198(8)	3277.2019(6)	3298.5455(6)
33	4.097	14447.6769(28)	3558.4534(24)	3600.6563(24)	3561.3595(21)	3558.6417(9)	3492.9789(6)	3514.8766(7)
34	4.140	15367.4898(31)	3787.9975(29)	3831.8504(28)	3790.9403(23)	3788.2282(10)	3715.6915(7)	3738.1493(8)
35	4.163	16317.0094(35)	4025.1299(33)	4070.6632(33)	4028.1039(25)	4025.4296(12)	3945.3434(9)	3968.3713(9)
36	4.188	17296.4192(40)	4269.9083(39)	4317.1536(39)	4272.9048(28)	4270.3027(13)	4181.9487(10)	4205.5535(10)
37	4.203	18305.8817(45)	4522.3843(45)	4571.3745(45)	4525.3963(31)	4522.9017(15)	4425.5121(11)	4449.7042(11)
38	4.220	19345.5859(50)	4782.6171(52)	4833.3863(52)	4785.6366(34)	4783.2864(17)	4676.0460(13)	4700.8341(13)
39	4.242	20415.7149(57)	5050.6650(60)	5103.2485(59)	5053.6844(37)	5051.5165(19)	4933.5584(15)	4958.9530(15)
40	4.270	21516.4668(55)	5326.5905(68)	5381.0250(68)	5329.6018(40)	5327.6554(20)	5198.0607(16)	5224.0715(16)
41	4.324	22648.0433(59)	5610.4577(77)	5666.7813(77)	5613.4528(44)	5611.7688(23)	5469.5645(18)	5496.2009(18)
42	4.409	23810.6519(62)	5902.3330(88)	5960.5850(88)	5905.3043(48)	5903.9244(25)	5748.0809(21)	5775.3522(21)
43	4.424	25004.531(17)	6202.287(10)	6262.509(10)	6205.2246(52)	6204.1909(28)	6033.6183(23)	6061.5361(23)
44	4.482	26229.8923(70)	6510.391(11)	6572.624(11)	6513.2865(57)	6512.6435(31)	6326.1923(26)	6354.7655(26)
45	4.494	27486.9801(75)	6826.721(13)	6891.009(13)	6829.5636(61)	6829.3559(34)	6625.8120(29)	6655.0515(29)
46	4.532	28776.0318(80)	7151.352(14)	7217.740(14)	7154.1338(67)	7154.4080(38)	6932.4920(32)	6962.4073(33)
47	4.544	30097.3149(85)	7484.366(16)	7552.902(16)	7487.0766(72)	7487.8800(42)	7246.2434(36)	7276.8451(36)
48	4.614	31451.0582(89)	7825.845(18)	7896.575(18)	7828.4762(78)	7829.8583(46)	7567.0825(40)	7598.3791(40)
49	4.617	32837.5878(96)	8175.878(20)	8248.854(20)	8178.4171(85)	8180.4275(51)	7895.0177(44)	7927.0210(45)
50	4.654	34257.139(10)	8534.551(22)	8609.825(22)	8536.9898(91)	8539.6807(56)	8230.0668(49)	8262.7860(49)
51	4.680	35710.024(11)	8901.957(24)	8979.582(24)	8904.2853(99)	8907.7097(61)	8572.2406(54)	8605.6870(54)
52	4.743	37196.518(12)	9278.192(26)	9358.224(26)	9280.402(11)	9284.6152(67)	8921.5582(60)	8955.7400(60)
53	4.750	38716.992(14)	9663.360(29)	9745.856(29)	9665.436(11)	9670.4938(73)	9278.0268(66)	9312.9573(66)
54	4.787	40271.720(16)	10057.560(32)	10142.578(32)	10059.495(12)	10065.4548(80)	9641.6688(72)	9677.3565(72)
55	4.804	41861.071(17)	10460.901(35)	10548.505(35)	10462.682(13)	10469.6042(87)	10012.4951(79)	10048.9515(79)
56	4.839	43485.362(19)	10873.493(38)	10963.744(38)	10875.111(14)	10883.0566(94)	10390.5244(87)	10427.7591(87)
57	4.855	45144.991(22)	11295.453(41)	11388.417(41)	11296.895(15)	11305.927(10)	10775.7699(95)	10813.7946(95)
58	4.877	46840.302(23)	11726.898(44)	11822.643(44)	11728.154(16)	11738.338(11)	11168.249(10)	11207.075(10)
59	4.892	48571.707(27)	12167.954(48)	12266.550(48)	12169.012(18)	12180.415(12)	11567.980(11)	11607.617(11)

TABLE VII. (*Continued.*)

Z	rms	$1\,^1S_0$	$2\,^1S_0$	$2\,^3S_1$	$2\,^3P_0$	$2\,^3P_1$	$2\,^1P_1$	$2\,^3P_2$
60	4.912	50339.584(28)	12618.747(52)	12720.266(52)	12619.597(19)	12632.289(13)	11974.978(12)	12015.438(12)
61	4.962	52144.29(13)	13079.400(59)	13183.918(59)	13080.042(20)	13094.094(14)	12389.262(13)	12430.556(13)
62	5.084	53986.108(37)	13550.033(60)	13657.626(60)	13550.485(22)	13565.972(15)	12810.851(15)	12852.989(15)
63	5.113	55865.914(39)	14030.847(65)	14141.597(65)	14031.071(23)	14048.068(17)	13239.759(16)	13282.754(16)
64	5.162	57783.891(41)	14521.952(69)	14635.942(69)	14521.948(25)	14540.534(18)	13676.008(17)	13719.872(17)
65	5.060	59741.10(58)	15023.59(11)	15140.91(11)	15023.273(27)	15043.530(20)	14119.615(18)	14164.359(18)
66	5.221	61736.549(50)	15535.696(79)	15656.424(79)	15535.201(28)	15557.211(21)	14570.602(20)	14616.238(20)
67	5.202	63772.42(15)	16058.688(87)	16182.923(87)	16057.906(30)	16081.757(22)	15028.985(22)	15075.526(21)
68	5.251	65848.240(61)	16592.584(90)	16720.420(89)	16591.557(32)	16617.337(24)	15494.787(23)	15542.245(23)
69	5.226	67965.248(67)	17137.671(95)	17269.208(95)	17136.339(34)	17164.142(26)	15968.028(25)	16016.416(25)
70	5.312	70123.037(79)	17693.98(10)	17829.32(10)	17692.432(36)	17722.353(28)	16448.730(27)	16498.060(27)
71	5.370	72322.90(22)	18261.82(11)	18401.06(11)	18260.034(39)	18292.173(30)	16936.911(29)	16987.197(29)
72	5.342	74565.930(87)	18841.45(11)	18984.72(11)	18839.356(41)	18873.816(32)	17432.596(31)	17483.851(31)
73	5.351	76852.016(97)	19432.98(12)	19580.38(12)	19430.601(44)	19467.488(34)	17935.805(33)	17988.042(33)
74	5.367	79181.93(10)	20036.63(13)	20188.28(12)	20033.992(47)	20073.415(36)	18446.562(35)	18499.795(35)
75	5.339	81556.90(17)	20652.72(13)	20808.75(13)	20649.763(49)	20691.838(39)	18964.890(38)	19019.133(38)
76	5.413	83976.20(12)	21281.25(14)	21441.77(14)	21278.140(52)	21322.983(41)	19490.813(40)	19546.080(40)
77	5.402	86442.5(1.3)	21922.77(26)	22087.93(26)	21919.390(58)	21967.125(47)	20024.353(43)	20080.658(43)
78	5.428	88955.17(15)	22577.32(15)	22747.25(15)	22573.763(59)	22624.515(47)	20565.536(46)	20622.894(46)
79	5.436	91515.81(17)	23245.29(16)	23420.13(16)	23241.535(63)	23295.437(50)	21114.387(49)	21172.811(49)
80	5.463	94124.69(18)	23926.85(16)	24106.75(16)	23922.987(66)	23980.176(53)	21670.931(52)	21730.437(52)
81	5.476	96783.19(20)	24622.39(17)	24807.51(17)	24618.420(70)	24679.038(57)	22235.193(56)	22295.796(55)
82	5.501	99491.84(21)	25332.14(18)	25522.63(18)	25328.141(74)	25392.336(60)	22807.201(59)	22868.917(59)
83	5.521	102251.76(24)	26056.44(18)	26252.48(18)	26052.477(79)	26120.401(64)	23386.979(63)	23449.823(63)
84	5.526	105064.30(39)	26795.70(20)	26997.45(19)	26791.774(83)	26863.588(68)	23974.556(67)	24038.543(66)
85	5.539	107930.0(1.4)	27550.16(32)	27757.81(32)	27546.382(91)	27622.252(76)	24569.961(71)	24635.107(70)
86	5.655	110847.35(55)	28319.72(22)	28533.44(22)	28316.637(93)	28396.733(76)	25173.224(75)	25239.546(75)
87	5.658	113823.03(52)	29105.74(22)	29325.74(22)	29103.011(98)	29187.516(81)	25784.368(79)	25851.881(79)
88	5.684	116854.73(97)	29908.00(27)	30134.49(27)	29905.87(10)	29994.968(87)	26403.426(84)	26472.146(84)
89	5.670	119945.7(2.2)	30727.28(45)	30960.47(45)	30725.67(12)	30819.564(99)	27030.427(89)	27100.369(88)
90	5.710	123094.1(2.1)	31563.44(45)	31803.55(44)	31562.83(12)	31661.71(10)	27665.406(94)	27736.588(93)
91	5.700	126304.8(2.6)	32417.56(53)	32664.84(53)	32417.87(13)	32521.97(11)	28308.383(99)	28380.820(99)
92	5.851	129570.30(64)	33288.51(24)	33543.15(24)	33291.14(13)	33400.67(11)	28959.41(10)	29033.12(10)
93	5.744	132911.0(3.2)	34180.26(64)	34442.59(64)	34183.55(15)	34298.74(13)	29618.49(11)	29693.49(11)
94	5.864	136305.1(2.4)	35088.99(50)	35359.21(50)	35095.18(15)	35216.27(13)	30285.68(12)	30361.98(12)
95	5.905	139769.54(75)	36018.13(25)	36296.53(25)	36026.93(15)	36154.18(12)	30961.00(12)	31038.63(12)
96	5.815	143310.9(4.2)	36969.20(86)	37256.14(85)	36979.57(19)	37113.26(17)	31644.49(13)	31723.45(13)
97	5.815	146916.9(4.6)	37940.11(94)	38235.86(94)	37953.43(21)	38093.82(19)	32336.19(14)	32416.50(14)
98	5.843	150592.6(5.1)	38932.1(1.0)	39237.0(1.0)	38949.28(23)	39096.68(20)	33036.12(14)	33117.81(14)
99	5.850	154343.9(5.6)	39946.7(1.2)	40261.0(1.1)	39967.97(25)	40122.69(23)	33744.33(15)	33827.41(15)
100	5.857	158171.1(6.1)	40984.1(1.3)	41308.3(1.3)	41010.25(27)	41172.62(25)	34460.86(16)	34545.33(16)

element $\langle \boldsymbol{p}_1 \cdot \boldsymbol{p}_2 \rangle$ taken from Ref. [18]. The known relativistic part of this correction of order $(\alpha Z)^4 m/M$ [76] was also included. The electron-electron interaction correction to the one-electron nuclear recoil was taken into account in the nonrelativistic limit. It was estimated as $(-m/M)\Delta E_{2\mathrm{el}}$, where $\Delta E_{2\mathrm{el}}$ is the total two-electron correction.

In the last column of Table VI we present the total values for the ionization energies, which are given by the sum of all corrections mentioned so far. For lead, thorium, and uranium, the total values include also the nuclear-polarization correction [77,78]. Analyzing the main sources of uncertainties listed in the table, we conclude that in the low-Z region the main error comes from the two-electron QED corrections, namely, from the two-photon exchange contribution. In the high-Z region, the main sources of uncertainty are the one-electron two-loop QED correction (mostly, the two-loop

TABLE VIII. Comparison of theoretical and experimental transition energies. Units are cm^{-1} or eV as noted.

Z	This work	Plante *et al.* [21]	Chen *et al.* [20]	Johnson *et al.* [19]	Experiment	Reference
			$2\,^3P_0$–$2\,^3S_1$ transition, in cm^{-1} unless specified			
12	95848(1)	95847	95848	95848	95851(7)	[80]
14	113809(2)	113809	113809	113809	113807(4)	[81]
					113815(4)	[82]
15	122956(2)	122955		122955	122953(9)	[81]
16	132220(2)	132219	132219	132219	132214(7)	[83]
					132198(10)	[82]
18	151158(3)	151155	151156	151155	151164(4)	[84]
					151204(9)	[85]
26	233484(10)	233469	233471		232558(550)	[86]
36	356891(39)	356822	356828	356823	357400(260)	[87]
92	252.01(27) eV	252.79	252.77		260.0(7.9)	[88]
			$2\,^3P_2$–$2\,^3S_1$ transition, in cm^{-1}			
12	100253(1)	100252	100253	100252	100263(6)	[80]
14	122744(1)	122743	122743	122743	122743(3)	[81]
					122746(3)	[82]
15	135154(1)	135151		135151	135150(5)	[81]
16	148499(1)	148496	148497	148496	148498(4)	[83]
					148493(5)	[82]
18	178581(2)	178576	178578	178576	178589(5)	[84]
					178591(31)	[85]
20	214179(2)	214170	214174	214170	214225(45)	[89]
22	256696(3)	256683	256688	256683	256746(46)	[90]
26	368767(6)	368742	368752	368742	368976(125)	[86]
28	441942(9)	441908	441920	441907	441950(80)	[91]
36	900116(33)	900009	900044	900008	900010(240)	[87]
			$2\,^3P_1$–$2\,^3S_1$ transition, in cm^{-1}			
12	96682(1)	96680	96681		96683(6)	[80]
13	106026(1)	106025			106023(7)	[80]
			$2\,^3P_1$–$2\,^1S_0$ transition, in cm^{-1}			
14	7229(2)	7231			7230.5(2)	[92]
			$2\,^3P_0$–$2\,^3P_1$ transition, in eV unless specified			
12	834(1) cm^{-1}	833	833		833.133(15)	[93]
28	2.324(1)	2.323	2.325		2.33(15)	[94]
47	0.803(8)	0.801	0.789		0.79(4)	[95]
64	18.586(31)	18.571	18.548		18.57(19)	[96]
			$1\,^1S_0$–$2\,^1P_1$ transition, in eV			
16	2460.629	2460.628			2460.649(9)	[97]
18	3139.582	3139.580			3139.553(38)	[98]
19	3510.462(1)	3510.459			3510.58(12)	[99]
21	4315.412(1)	4315.409			4315.54(15)	[99]
22	4749.644(1)	4749.639			4749.74(17)	[99]
23	5205.165(1)	5205.154			5205.27(21)	[99]
					5205.10(14)	[100]
24	5682.068(1)	5682.061			5682.32(40)	[99]
26	6700.435(1)	6700.423			6700.73(20)	[99]
					6700.90(25)	[101]
32	10280.218(3)	10280.185			10280.70(22)	[102]

TABLE VIII. (*Continued.*)

Z	This work	Plante *et al.* [21]	Chen *et al.* [20]	Johnson *et al.* [19]	Experiment	Reference
36	13114.470(4)	13114.411			13115.31(30)	[103]
					13114.68(36)	[104]
54	30630.051(17)	30629.667			30629.1(3.5)	[105]
92	100610.89(65)	100613.924			100626(35)	[106]
			$1\,^1S_0$–$2\,^3P_1$, in eV			
18	3123.534	3123.532			3123.522(36)	[98]
23	5180.326(1)	5180.327			5180.22(17)	[100]
26	6667.579(1)	6667.564			6667.50(25)	[101]
32	10220.800(3)	10220.759			10221.80(35)	[102]
36	13026.117(4)	13026.044			13026.8(3)	[103]
54	30206.265(18)	30205.852			30209.6(3.5)	[105]
92	96169.63(65)	96172.427			96171(52)	[106]
			$1\,^1S_0$–$2\,^3P_2$, in eV			
23	5188.738(1)	5188.730			5189.12(21)	[100]
			$1\,^1S_0$–$2\,^3S_1$, in eV			
23	5153.896(1)	5153.889			5153.82(14)	[100]

self-energy correction) and the experimental values for the rms nuclear radii.

In Table VII, the total ionization energies of $n=1$ and 2 states of He-like ions with $Z=12$–100 are listed. We start our compilation with $Z=12$ since this is the point where the additional terms accounted for in our calculation $[\sim\alpha^2(\alpha Z)^4]$ become comparable with omitted higher-order effects $[\sim\alpha^3(\alpha Z)^2]$.

In Fig. 5, our results are compared with the theoretical values obtained previously in calculations of different types [18,21,24]. Since our evaluation is the first one complete to the order $\alpha^2(\alpha Z)^4$, it is interesting to analyze the difference between various calculations in units of $\alpha^2(\alpha Z)^4$. First of all, we note a significant deviation of our values from the recent results by Cheng and Chen [24], which arises from an incomplete treatment of QED corrections employed in that work. The authors evaluate the QED correction to all orders in αZ at the one-loop level, employing a symmetric model potential in order to account for the electron-electron interaction. This approximation works reasonably well in the high-Z region, but for ions with $22\leqslant Z\leqslant 36$ (as presented in the paper), the accuracy of this approximation turns out to be lower than that of Drake's approach based on the exact αZ expansion [18]. We mention that a previous investigation by these authors [20] employed the QED correction as evaluated by Drake. Its results agree well with those by Plante *et al.* [21] and thus are in a better agreement with our numerical values.

For the $^1S_0$ and $2\,^3P_{0,1}$ states, we observe also a distinct deviation of our ionization energies from the results by Drake [18]. A similar deviation was reported previously in the literature [19–21], where it was attributed to corrections of order $\alpha^2(\alpha Z)^4$ to the electron-electron interaction that were not accounted for by Drake's unified method but can be (to a certain extent) included by methods based on the no-pair QED Hamiltonian [79]. Irregularities of the Z dependence of the plotted difference, which can be observed for S states in the medium- and high-Z region, are explained by more recent values for the rms nuclear radii employed in the present calculation.

As can be seen from Fig. 5, the best agreement is found with the calculation by Plante *et al.* [21]. It is to be noted that the results by Johnson and Sapirstein [19] and by Chen *et al.* [20] obtained by different methods but on the same level of sophistication are in a very good agreement with the ones by Plante and co-workers. Whereas all these results are incomplete to order $\alpha^2(\alpha Z)^4$, we conclude that the remaining contribution of this order is rather small for all $n=2$ states, which explains the good agreement of these results with the experimental data. Only for the $1\,^1S_1$ state do we observe a significant additional contribution of about $0.5\ \alpha^2(\alpha Z)^4$. We mention, however, that despite the good agreement observed for the $n=2$ states, the results by Plante *et al.* are well outside the estimated error bars of the present theoretical values for most middle- and high-Z ions.

In Table VIII, we list transition energies for which experimental results are available. Comparison is made with the MBPT calculation by Johnson and Sapirstein [19], with the CI calculations by Chen *et al.* [20], and with the all-order many-body treatment by Plante *et al.* [21]. These studies are, according to our analysis, the most complete ones among the previous calculations. We recall that in all these investigations QED corrections were taken as evaluated by Drake [18]. The difference between them, therefore, is related only to the part arising from the no-pair Hamiltonian, often referred to as the "structure" part.

We observe a generally good agreement of theoretical predictions with experimental data. Despite the significant amount of available experimental information, the experimental uncertainty in the region of Z under consideration is generally larger than the difference between the calculations analyzed in Table VIII. Among few exceptions are the recent high-precision measurements of the $2\,^3P_1$–$2\,^1S_0$ transition

TABLE IX. The $2\,^3P_0$–$2\,^1S_0$ energy difference, in eV.

	$Z=63$	$Z=64$	$Z=65$	$Z=66$	$Z=89$	$Z=90$	$Z=91$	$Z=92$
This work	−0.224(69)	0.004(74)	0.32(12)	0.495(84)	1.61(46)	0.61(46)	−0.31(55)	−2.64(28)
Andreev *et al.* [42]	−0.591	−0.389	−0.153	0.016			−1.971	−4.511
Plante *et al.* [21]		−0.170		0.341		−0.095		−2.639
Drake [18]	−0.168	0.067	0.328	0.614	1.731	0.718	−0.209	−1.816
Maul *et al.* [12]								0.30

energy in silicon ($Z=14$) [92] and the $2\,^3P_0$–$2\,^3P_1$ transition energy in magnesium ($Z=12$) [93], whose accuracy is much higher than that of the theoretical predictions. However, at these relatively low values of Z, our treatment is basically equivalent to the previous studies, and the difference between the calculations cannot be effectively probed in comparison with these measurements. When Z increases, deviation of our values from the results of the previous studies becomes more prominent, but the experimental uncertainty is much lower for higher Z. A compromise is found to be argon ($Z=18$), where the experimental determination of the $2\,^3P_{0,2}$–$2\,^3S_1$ transition energies by Kukla *et al.* [84] demonstrated a 2σ deviation from the previous theoretical results. Our calculation brings the theoretical and experimental results into agreement for the $2\,^3P_0$–$2\,^3S_1$ transition and reduces the discrepancy for the $2\,^3P_2$–$2\,^3S_1$ transition to 0.5σ.

An important feature of He-like ions is that they provide a possibility to study the effects of parity nonconservation [10,11]. The $2\,^1S_0$–$2\,^3P_0$ transition in the He-like Eu ion ($Z=63$) is presently considered as the best candidate for future experiments [13]. The effect is enhanced by the fact that the $2\,^1S_0$ and $2\,^3P_0$ levels cross each other in the vicinity of $Z=63$. Another crossing point of the levels occurs around $Z=90$. The energy difference for ions near this crossing point can be, in principle, reduced even further by choosing the appropriate isotope [12]. In Table IX we list the results of different theoretical evaluations for the $2\,^3P_0$–$2\,^1S_0$ energy difference in ions near the crossing points. A significant discrepancy is observed between different theoretical evaluations, which is due to the smallness of the energy difference for these ions. We mention a significant deviation of our values from the recent results by Andreev *et al.* [42]. In that work, the authors performed an *ab initio* calculation of the two-photon exchange correction, whose numerical values agree well with those obtained in this paper. However, evaluating the total transition energy, the authors used an estimation for the screened self-energy correction (that was not calculated at that moment), which is the main source of the disagreement observed.

SUMMARY

In this investigation we performed *ab initio* QED calculations of the screened self-energy correction and the two-photon exchange correction for $n=1$ and 2 states of He-like ions with $Z\geqslant 12$. This evaluation completes the rigorous treatment of all *two-electron* QED corrections of order α^2 to all orders in αZ and significantly improves the theoretical accuracy for the energy values, especially in the high-Z region. Unlike previous calculations, the results obtained are complete through order $\alpha^2(\alpha Z)^4$; uncalculated terms enter through three-photon-exchange QED effects [$\sim\alpha^3(\alpha Z)^2$ and higher] and through higher-order one-electron two-loop QED corrections [$\sim\alpha^2(\alpha Z)^7$ and higher].

ACKNOWLEDGMENTS

Stimulating discussions with P. Mohr, J. Sapirstein, and T. Stöhlker are gratefully acknowledged. This work was supported in part by RFBR (Grant No. 04-02-17574), by the Russian Ministry of Education (Grant No. E02-3.1-49), and by INTAS-GSI (Grant No. 03-54-3604). The work of V.M.S. was supported by the Alexander von Humboldt Stiftung. A.N.A. and V.A.Y. acknowledge support by the "Dynasty" foundation. The work of A.N.A. was also supported by INTAS YS Grant No. 03-55-960 and by Russian Ministry of Education and Administration of St. Petersburg (Grant No. PD02-1.2-79). G.P. and G.S. acknowledge financial support by the BMBF, DFG, and GSI.

[1] H. Araki, Prog. Theor. Phys. **17**, 619 (1957).
[2] J. Sucher, Phys. Rev. **109**, 1010 (1958).
[3] G. W. F. Drake, in *The Hydrogen Atom. Precision Physics of Simple Atomic Systems*, edited by S. G. Karshenboim *et al.* (Springer, Berlin, 2001), p. 57.
[4] K. Pachucki, Phys. Rev. Lett. **84**, 4561 (2000).
[5] V. Korobov and A. Yelkhovsky, Phys. Rev. Lett. **87**, 193003 (2001).
[6] K. Pachucki, J. Phys. B **35**, 3087 (2002).
[7] R. E. Marrs, S. R. Elliott, and T. Stöhlker, Phys. Rev. A **52**, 3577 (1995).
[8] T. Stöhlker, S. R. Elliot, and R. E. Marrs, Hyperfine Interact. **99**, 217 (1996).
[9] A. Gumberidze, T. Stohlker, D. Banas, K. Beckert, P. Beller, H. F. Beyer, F. Bosch, X. Cai, S. Hagmann, C. Kozhuharov, D. Liesen, F. Nolden, X. Ma, P. H. Mokler, A. Orsic-Muthig, M. Steck, D. Sierpowski, S. Tashenov, A. Warczak, and Y. Zou, Phys. Rev. Lett. **92**, 203004 (2004).

[10] A. Schäfer, G. Soff, P. Indelicato, B. Müller, and W. Greiner, Phys. Rev. A **40**, 7362 (1989).
[11] V. Karasiev, L. Labzowsky, and A. Nefiodov, Phys. Lett. A **172**, 62 (1992).
[12] M. Maul, A. Schäfer, W. Greiner, and P. Indelicato, Phys. Rev. A **53**, 3915 (1996).
[13] L. N. Labzowsky, A. V. Nefiodov, G. Plunien, G. Soff, R. Marrus, and D. Liesen, Phys. Rev. A **63**, 054105 (2001).
[14] P. J. Mohr, Ann. Phys. (N.Y.) **88**, 26 (1974); **88**, 52 (1974).
[15] G. Soff and P. J. Mohr, Phys. Rev. A **38**, 5066 (1988).
[16] P. J. Mohr, Nucl. Instrum. Methods Phys. Res. B **9**, 459 (1985).
[17] P. Indelicato, O. Gorceix, and J. Desclaux, J. Phys. B **20**, 651 (1987).
[18] G. W. F. Drake, Can. J. Phys. **66**, 586 (1988).
[19] W. R. Johnson and J. Sapirstein, Phys. Rev. A **46**, R2197 (1992).
[20] M. H. Chen, K. T. Cheng, and W. R. Johnson, Phys. Rev. A **47**, 3692 (1993).
[21] D. R. Plante, W. R. Johnson, and J. Sapirstein, Phys. Rev. A **49**, 3519 (1994).
[22] P. Indelicato, Phys. Rev. A **51**, 1132 (1995).
[23] K. T. Cheng, M. H. Chen, W. R. Johnson, and J. Sapirstein, Phys. Rev. A **50**, 247 (1994).
[24] K. T. Cheng and M. H. Chen, Phys. Rev. A **61**, 044503 (2000).
[25] S. A. Blundell, P. J. Mohr, W. R. Johnson, and J. Sapirstein, Phys. Rev. A **48**, 2615 (1993).
[26] I. Lindgren, H. Persson, and S. Salomonson, and L. Labzowsky, Phys. Rev. A **51**, 1167 (1995).
[27] H. Persson, S. Salomonson, P. Sunnergren, and I. Lindgren, Phys. Rev. Lett. **76**, 204 (1996).
[28] A. N. Artemyev, V. M. Shabaev, and V. A. Yerokhin, Phys. Rev. A **56**, 3529 (1997).
[29] V. A. Yerokhin, A. N. Artemyev, and V. M. Shabaev, Phys. Lett. A **234**, 361 (1997).
[30] A. N. Artemyev, T. Beier, G. Plunien, V. M. Shabaev, G. Soff, and V. A. Yerokhin, Phys. Rev. A **60**, 45 (1999).
[31] V. A. Yerokhin, A. N. Artemyev, T. Beier, G. Plunien, V. M. Shabaev, and G. Soff, Phys. Rev. A **60**, 3522 (1999).
[32] V. A. Yerokhin, A. N. Artemyev, V. M. Shabaev, M. M. Sysak, O. M. Zherebtsov, and G. Soff, Phys. Rev. Lett. **85**, 4699 (2000); Phys. Rev. A **64**, 032109 (2001).
[33] J. Sapirstein and K. T. Cheng, Phys. Rev. A **64**, 022502 (2001).
[34] V. M. Shabaev, Teor. Mat. Fiz. **82**, 83 (1990) [Theor. Math. Phys. **82**, 57 (1990)].
[35] V. M. Shabaev, J. Phys. B **26**, 4703 (1993).
[36] V. M. Shabaev, Phys. Rep. **356**, 119 (2002).
[37] I. Lindgren, B. Åsen, S. Salomonson, and A.-M. Mårtensson-Pendrill, Phys. Rev. A **64**, 062505 (2001).
[38] O. Y. Andreev, L. N. Labzowsky, G. Plunien, and G. Soff, Phys. Rev. A **69**, 062505 (2004).
[39] A. N. Artemyev, T. Beier, G. Plunien, V. M. Shabaev, G. Soff, and V. A. Yerokhin, Phys. Rev. A **62**, 022116 (2000).
[40] P. J. Mohr and J. Sapirstein, Phys. Rev. A **62**, 052501 (2000).
[41] O. Y. Andreev, L. N. Labzowsky, G. Plunien, and G. Soff, Phys. Rev. A **64**, 042513 (2001).
[42] O. Y. Andreev, L. N. Labzowsky, G. Plunien, and G. Soff, Phys. Rev. A **67**, 012503 (2003).
[43] B. Åsen, S. Salomonson, and I. Lindgren, Phys. Rev. A **65**, 032516 (2002).
[44] P. Indelicato and P. J. Mohr, Phys. Rev. A **63**, 052507 (2001).
[45] V. M. Shabaev, Phys. Rev. A **50**, 4521 (1994).
[46] C. Itzykson and J. B. Zuber, *Quantum Field Theory* (McGraw-Hill, New York, 1980).
[47] M. H. Mittleman, Phys. Rev. A **5**, 2395 (1972).
[48] V. M. Shabaev and I. G. Fokeeva, Phys. Rev. A **49**, 4489 (1994).
[49] E.-O. Le Bigot, P. Indelicato, and V. M. Shabaev, Phys. Rev. A **63**, 040501(R) (2001).
[50] A. N. Artemyev, V. M. Shabaev, M. M. Sysak, V. A. Yerokhin, T. Beier, G. Plunien, and G. Soff, Phys. Rev. A **67**, 062506 (2003).
[51] V. A. Yerokhin, P. Indelicato, and V. M. Shabaev, Eur. Phys. J. D **25**, 203 (2003).
[52] P. Sunnergren, Ph.D. thesis, Göteborg University and Chalmers University of Technology, 1998 (unpublished).
[53] F. C. Sanders and C. W. Scherr, Phys. Rev. **181**, 84 (1969).
[54] K. Aashamar, G. Lyslo, and J. Midtdal, J. Chem. Phys. **52**, 3324 (1970).
[55] S. P. Goldman and G. W. F. Drake, J. Phys. B **17**, L197 (1984).
[56] G. W. F. Drake, Nucl. Instrum. Methods Phys. Res. B **202**, 273 (1982).
[57] V. M. Shabaev, J. Phys. B **26**, 1103 (1993).
[58] I. Angeli, At. Data Nucl. Data Tables **87**, 185 (2004).
[59] W. R. Johnson and G. Soff, At. Data Nucl. Data Tables **33**, 405 (1985).
[60] P. J. Mohr and B. N. Taylor, Rev. Mod. Phys. **77**, 1 (2005).
[61] T. Beier, P. J. Mohr, H. Persson, and G. Soff, Phys. Rev. A **58**, 954 (1998).
[62] P. J. Mohr and Y.-K. Kim, Phys. Rev. A **45**, 2727 (1992).
[63] P. J. Mohr and G. Soff, Phys. Rev. Lett. **70**, 158 (1993).
[64] P. J. Mohr, Phys. Rev. A **46**, 4421 (1992).
[65] T. Beier, G. Plunien, M. Greiner, and G. Soff, J. Phys. B **30**, 2761 (1997).
[66] A. G. Fainshtein, N. L. Manakov, and A. A. Nekipelov, J. Phys. B **24**, 559 (1991).
[67] P. J. Mohr and B. N. Taylor, Rev. Mod. Phys. **72**, 351 (2000).
[68] K. Pachucki, Phys. Rev. A **63**, 042503 (2001).
[69] K. Pachucki and U. D. Jentschura, Phys. Rev. Lett. **91**, 113005 (2003).
[70] U. D. Jentschura, Phys. Rev. A **70**, 052108 (2004).
[71] V. A. Yerokhin, P. Indelicato, and V. M. Shabaev, Phys. Rev. A **71**, 040101(R) (2005).
[72] K. Pachucki (private communication).
[73] A. N. Artemyev, V. M. Shabaev, and V. A. Yerokhin, Phys. Rev. A **52**, 1884 (1995).
[74] A. N. Artemyev, V. M. Shabaev, and V. A. Yerokhin, J. Phys. B **28**, 5201 (1995).
[75] V. M. Shabaev, A. N. Artemyev, T. Beier, G. Plunien, V. A. Yerokhin, and G. Soff, Phys. Rev. A **57**, 4235 (1998).
[76] V. M. Shabaev and A. N. Artemyev, J. Phys. B **27**, 1307 (1994).
[77] G. Plunien and G. Soff, Phys. Rev. A **51**, 1119 (1995); **53**, 4614(E) (1996).
[78] A. V. Nefiodov, L. N. Labzowsky, G. Plunien, and G. Soff, Phys. Lett. A **222**, 227 (1996).
[79] J. Sucher, Phys. Rev. A **22**, 348 (1980).
[80] H. A. Klein, F. Moscatelli, E. G. Myers, E. H. Pinnington, J. D.

Silver, and, E. Träbert, J. Phys. B **18**, 1483 (1985).
[81] D. J. H. Howie, W. A. Hallett, E. G. Myers, D. D. Dietrich, and J. D. Silver, Phys. Rev. A **49**, 4390 (1994); D. J. H. Howie, J. D. Silver, and E. G. Myers, *ibid.* **52**, 1761 (1995).
[82] R. DeSerio, H. G. Berry, R. L. Brooks, J. Hardis, A. E. Livingston, and S. J. Hinterlong, Phys. Rev. A **24**, 1872 (1981).
[83] D. J. H. Howie, J. D. Silver, and E. G. Myers, J. Phys. B **29**, 927 (1996).
[84] K. W. Kukla, A. E. Livingston, J. Suleiman, H. G. Berry, R. W. Dunford, D. S. Gemmell, E. P. Kanter, S. Cheng, and L. J. Curtis, Phys. Rev. A **51**, 1905 (1995).
[85] H. F. Beyer, F. Folkmann, and K. H. Schartner, Z. Phys. D: At., Mol. Clusters **1**, 65 (1986).
[86] J. P. Buchet, M. C. Buchet-Poulizac, A. Denis, J. Desesquelles, M. Druetta, J. P. Grandin, and X. Husson, Phys. Rev. A **23**, 3354 (1981).
[87] S. Martin, A. Denis, M. C. Buchet-Poulizac, J. P. Buchet, and J. Desesquelles, Phys. Rev. A **42**, 6570 (1990).
[88] C. T. Munger and H. Gould, Phys. Rev. Lett. **57**, 2927 (1986).
[89] S. J. Hinterlong and A. E. Livingston, Phys. Rev. A **33**, 4378 (1986).
[90] E. J. Galvez, A. E. Livingston, A. J. Mazure, H. G. Berry, L. Engström, J. E. Hardis, L. P. Somerville, and D. Zei, Phys. Rev. A **33**, 3667 (1986).
[91] A. S. Zacarias, A. E. Livingston, Y. N. Lu, R. F. Ward, H. G. Berry, and R. W. Dunfors, Nucl. Instrum. Methods Phys. Res. B **31**, 41 (1988).
[92] M. Redshaw and E. G. Myers, Phys. Rev. Lett. **88**, 023002 (2002).
[93] E. G. Myers and M. R. Tarbutt, in *The Hydrogen Atom: Precision Physics of Simple Atomic Systems*, edited by S. G. Karshenboim *et al.* (Springer, Berlin, 2001), p. 679.
[94] R. W. Dunford, C. J. Liu, J. Last, N. Berrah-Mansour, R. Vondrasek, D. A. Church, and L. J. Curtis, Phys. Rev. A **44**, 764 (1991).
[95] B. B. Birkett, J.-P. Briand, P. Charles, D. D. Dietrich, K. Finlayson, P. Indelicato, D. Liesen, R. Marrus, and A. Simionovici, Phys. Rev. A **47**, R2454 (1993); R. Marrus, A. Simionovici, P. Indelicato, D. D. Dietrich, P. Charles, J. P. Briand, K. Finlayson, F. Bosch, D. Liesen, and F. Parente, Phys. Rev. Lett. **63**, 502 (1989).
[96] P. Indelicato, B. B. Birkett, J.-P. Briand, P. Charles, D. D. Dietrich, R. Marrus, and A. Simionovici, Phys. Rev. Lett. **68**, 1307 (1992).
[97] L. Schleinkofer, F. Bell, H.-D. Betz, G. Trollmann, and J. Rothermel, Phys. Scr. **25**, 917 (1982).
[98] R. D. Deslattes, H. F. Beyer, and F. Folkmann, J. Phys. B **17**, L689 (1984).
[99] P. Beiersdorfer, M. Bitter, S. vonGoeler, and K. W. Hill, Phys. Rev. A **40**, 150 (1989).
[100] C. T. Chantler, D. Paterson, L. T. Hudson, F. G. Serpa, J. D. Gillaspy, and E. Takács, Phys. Rev. A **62**, 042501 (2000).
[101] J. P. Briand, M. Tavernier, R. Marrus, and J. P. Desclaux, Phys. Rev. A **29**, 3143 (1984).
[102] S. MacLaren, P. Beiersdorfer, D. A. Vogel, D. Knapp, R. E. Marrs, K. Wong, and R. Zasadzinski, Phys. Rev. A **45**, 329 (1992).
[103] P. Indelicato, J. P. Briand, M. Tavernier, and D. Liesen, Z. Phys. D: At., Mol. Clusters **2**, 249 (1986).
[104] K. Widmann, P. Beiersdorfer, V. Decaux, and M. Bitter, Phys. Rev. A **53**, 2200 (1996).
[105] J. P. Briand, P. Indelicato, A Simionovici, V. San Vicente, D. Liesen, and D. Dietrich, Europhys. Lett. **9**, 225 (1989).
[106] J. P. Briand, P. Chevallier, P. Indelicato, K. P. Ziock, and D. D. Dietrich, Phys. Rev. Lett. **65**, 2761 (1990).